NOW SHIPPING!

MultiMet-WL Cube

The latest addition to the Sun Nuclear SRS QA Portfolio

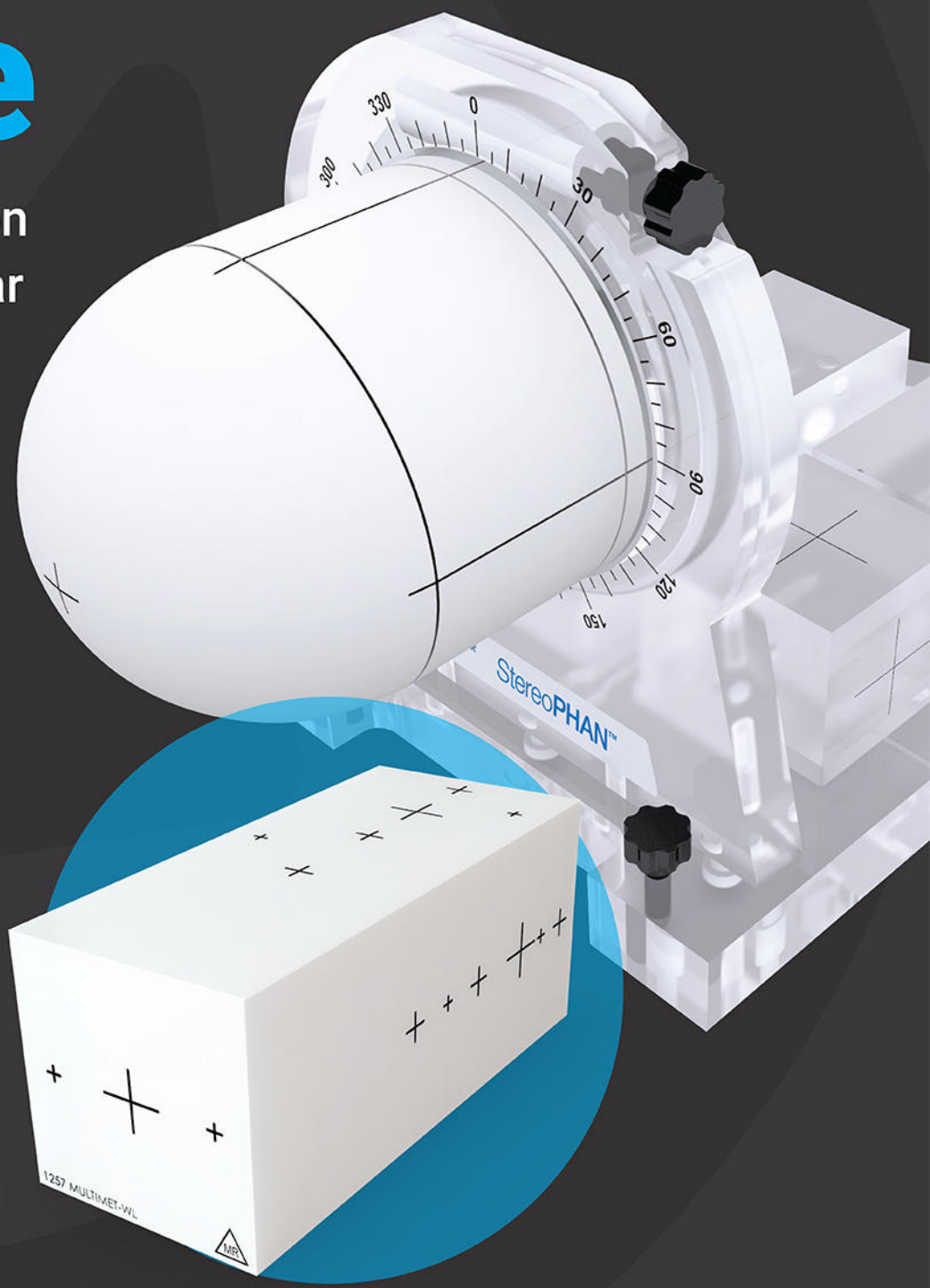

Quantify the margin of error for off-axis SRS targets. Use with StereoPHAN™ or as a standalone phantom.

Learn More

SUN NUCLEAR corporation

Task Group 174 Report: Utilization of [^{18}F]Fluorodeoxyglucose Positron Emission Tomography ([^{18}F]FDG-PET) in Radiation Therapy

Shiva K. Das[a], and Ross McGurk
Department of Radiation Oncology, University of North Carolina School of Medicine, Chapel Hill, NC, USA

Moyed Miften
Department of Radiation Oncology, University of Colorado School of Medicine, Aurora, CO, USA

Sasa Mutic
Department of Radiation Oncology, Washington University School of Medicine, St. Louis, MO, USA

James Bowsher
Department of Radiation Oncology, Duke University Medical Center, Durham, NC, USA

John Bayouth
Human Oncology, University of Wisconsin, Madison, WI, USA

Yusuf Erdi
Department of Medical Physics, Memorial Sloan-Kettering Cancer Center, New York, NY, USA

Osama Mawlawi
Department of Imaging Physics, University of Texas, M D Anderson Cancer Center, Houston, TX, USA

Ronald Boellaard
Department of Radiology and Nuclear Medicine, VU University Medical Center, Amsterdam, The Netherlands

Stephen R. Bowen
Department of Radiation Oncology, University of Washington, Seattle, WA, USA

Lei Xing
Department of Radiation Oncology, Stanford University School of Medicine, Stanford, CA, USA

Jeffrey Bradley
Department of Radiation Oncology, Washington University School of Medicine, St. Louis, MO, USA

Heiko Schoder
Molecular Imaging and Therapy Service, Memorial Sloan-Kettering Cancer Center, New York, NY, USA

Fang-Fang Yin
Department of Radiation Oncology, Duke University Medical Center, Durham, NC, USA

Daniel C. Sullivan
Department of Radiology, Duke University School of Medicine, Durham, NC, USA

Paul Kinahan
Department of Radiology, University of Washington, Seattle, WA, USA

(Received 6 April 2019; revised 30 April 2019; accepted for publication 6 June 2019; published xx xxxx xxxx)

The use of positron emission tomography (PET) in radiation therapy (RT) is rapidly increasing in the areas of staging, segmentation, treatment planning, and response assessment. The most common radiotracer is ^{18}F-fluorodeoxyglucose ([^{18}F]FDG), a glucose analog with demonstrated efficacy in cancer diagnosis and staging. However, diagnosis and RT planning are different endeavors with unique requirements, and very little literature is available for guiding physicists and clinicians in the utilization of [^{18}F]FDG-PET in RT. The two goals of this report are to educate and provide recommendations. The report provides background and education on current PET imaging systems, PET tracers, intensity quantification, and current utilization in RT (staging, segmentation, image registration, treatment planning, and therapy response assessment). Recommendations are provided on acceptance testing, annual and monthly quality assurance, scanning protocols to ensure consistency between interpatient scans and intrapatient longitudinal scans, reporting of patient and scan parameters in literature, requirements for incorporation of [^{18}F]FDG-PET in treatment planning systems, and image registration. The recommendations provided here are minimum requirements and are not meant to cover all aspects of the use of [^{18}F]FDG-PET for RT. [https://doi.org/10.1002/mp.13676]

Key words: FDG-PET, protocols, quality assurance, radiation therapy

1. Introduction
2. Current usage of [^{18}F]FDG-PET in RT
2.A. Current PET imaging systems
2.A.1. PET imaging technology
2.A.2. PET only and PET/CT clinical RT applications
2.A.3. PET tracers
2.B. [^{18}F]FDG-PET quantification using Standardized Uptake Value (SUV)
2.C. Utilization of [^{18}F]FDG-PET in RT
2.C.1. Staging
2.C.2. Segmentation
2.C.3. Image registration
2.C.4. Respiratory gating
2.C.5. Treatment planning
2.C.6. Therapy response assessment
3. Recommendations for consistency of [^{18}F]FDG-PET usage in RT
3.A. Acceptance testing and quality assurance
3.A.1. Acceptance testing
3.A.2. Annual QA
3.A.3. Monthly QA and Daily QA
3.B. Scanning protocol
3.C. Reporting in literature
3.D. Treatment planning system [^{18}F]FDG-PET-specific requirements
3.E. Image registration
3.F. Radiation dose to patients and staff
4. Summary of recommendations

1. INTRODUCTION

Accurate delivery of Radiation Therapy (RT) is critical for long-term survival of cancer patients. Central to RT is tumor segmentation, such that it may be maximally targeted to achieve local control and limit the irradiation of surrounding normal tissue. Typically, RT planning is based on computed tomography (CT)-based anatomical imaging. Due to excellent spatial resolution and ability to provide electron density information, CT has been the backbone of RT planning. However, lack of sufficient contrast resolution and functional information can lead to inadequate information on the tumor spatial extents. This limitation leads to large variability in defining the extent of disease, regardless of the specific disease site.[1–9] To address those limitations, other imaging exams are frequently incorporated to complement CT images. One such imaging system is Positron emission tomography (PET), which utilizes radioactive tracers to provide an image of tissue biological activity. In this way, higher concentrations of activity within actual/suspected neoplastic tissues are displayed with higher intensities than surrounding normal tissues. In the context of this report, higher intensities of ^{18}F-fluorodeoxyglucose ([^{18}F]FDG) are used to identify regions of higher metabolism, typically associated with cancerous tissue. Recent studies have noted improved sensitivity and specificity of cancer staging; for example, the sensitivity and specificity of mediastinal lymph node metastasis identification in non-small cell lung cancer was 77% and 86% with PET/CT, respectively, as compared to only 55% and 81% for CT alone.[10] However, it should be noted that [^{18}F]Fluorodeoxyglucose-PET ([^{18}F]FDG-PET) can be taken up by normal tissues as well, so care in image interpretation by qualified physicians is essential.

While [^{18}F]FDG-PET imaging has demonstrated notable success in visualizing tumor metabolic activity, it is routinely used in conjunction with CT to render combined anatomic and functional information. CT additionally provides information for attenuation correction of the PET signal.[11] [^{18}F]FDG-PET/CT has been shown to change the extent of disease identification and delineation in 15%–20% of cancer patients compared to CT alone in a retrospective analysis.[12] Consequently, [^{18}F]FDG-PET/CT-guided RT planning has seen increasing use in head and neck cancer,[13] lung cancer,[14–16] breast cancer,[17,18] esophageal cancer,[19] non-Hodgkin's lymphoma,[20] gynecologic cancer,[21] rectal cancer,[22] and anal cancer.[23] The advantages of combined anatomic and functional imaging have led to widespread adoption of PET/CT in RT clinics.[24] The growth in the number of PET/CT scanners in the Unites States increased approximately tenfold in a decade,[25] from approximately 200 in 2001 to more than 2500 in 2013.[26] Approximately 4% of the PET procedures were for RT treatment planning.[27] Based on the increasing use of [^{18}F]FDG-PET in RT, this percentage contribution is likely to steadily increase. [^{18}F]FDG-PET/CT has three major current applications in RT clinics: (a) to identify and stage disease; (b) to improve delineation of metabolically active target tissue (tumor and nodes); and (c) to assess tumor response to RT.

Notwithstanding increased adoption, there is no consensus on a standard protocol for the clinical use of [^{18}F]FDG-PET in the context of RT, though recommendations have been made on various aspects[28,29] [also see special issue — *Radiotherapy and Oncology*: PET in Radiotherapy Planning, 96(3), 2010]. A standard protocol is imperative not only for safe patient treatment but also to ensure intraclinic and interclinic standardization of implementation. For example, data on the variances and biases inherent in quantifying [^{18}F]FDG-PET tracer uptake are needed to ascertain the significance of any measured differences, such as in quantifying response to therapy. Cognizant of the lack of consensus, European guidelines were published in 2010 and provide recommendations for harmonization of quantitative PET/CT scans.[30]

The charge of this task group is as follows:

> "To recommend guidelines/protocols for consistent imaging, consistent treatment planning, and consistent treatment assessment using FDG-PET in radiotherapy. This report is envisioned as laying the foundation for standardizing the use of FDG-PET in radiotherapy. The guidelines/protocols will facilitate interpretability of results and interinstitutional translatability of radiotherapy techniques involving FDG-PET. Toward this goal, this task group will deal with the issues of methods of hypermetabolic target delineation, quality assurance/assessment of FDG-PET scans in phantoms, future FDG-PET software tools

required within radiotherapy treatment planning systems, and patient preparation and imaging parameters." Based on the official charge, the two goals of this report are to educate and provide recommendations:

- The report provides background and education on current PET imaging systems, PET tracers, intensity quantification, and current utilization in RT (staging, segmentation, image registration, treatment planning, and therapy response assessment).
- Recommendations are provided on acceptance testing, annual and monthly quality assurance, scanning protocols to ensure consistency between interpatient scans and intrapatient longitudinal scans, reporting of patient and scan parameters in literature, requirements for incorporation of [^{18}F]FDG-PET in treatment planning systems, and image registration. The recommendations provided here are not meant to replace procedures established at individual institutions that go above and beyond the recommendations.

The procedures outlined in this report are meant to be performed by a Qualified Medical Physicist (QMP) (refer to American Association of Physicists in Medicine (AAPM) "Definition of a Qualified Medical Physicist"[31]), as appropriate, or individuals working under the general supervision of a QMP ("general supervision" as defined in the AAPM Medical Physics Practice Guideline[32]). The documentation of work should be signed by all individuals performing the work, including the supervising QMP.

The quantitative accuracy of PET imaging is governed by: (a) accurate scanner calibration; (b) image quality; and (c) processes for ensuring that images are acquired in a consistent manner. This report only addresses item (c). Items (a) and (b), also crucial to quantitative PET imaging, lie squarely in the realm of Nuclear Medicine and may only be ensured by a QMP. Failure of any of the tests outlined in this Task Group report may only be corrected via remedial actions by a QMP or individuals working under the supervision of a QMP.

2. CURRENT USAGE OF [^{18}F]FDG-PET IN RT

2.A. Current PET imaging systems

2.A.1. PET imaging technology

PET imaging relies on positron-emitting radionuclides that are tagged to pharmaceutical agents and intravenously injected, where they bind to receptor sites or become incorporated into a biological process. PET is therefore inherently a functional or biological imaging modality. PET imaging is essentially the time-coincident detection of the two annihilation photons emitted when a positron and electron interact. Upon radioactive decay, an emitted positron will interact with a surrounding electron and annihilate, producing two 511 keV photons emitted approximately 180° apart from each other. The detection of these photons is typically achieved by stationary scintillating crystals arranged in a 360° ring around the patient. Modern commercial PET scanners rely on higher density crystals such as bismuth germanate (BGO), lutetium oxyorthsilicate (LSO), and lutetium yttrium oxyorthsilicate (LYSO).

PET relies on coincident detection of the photons created from the annihilation of a single positron, a process known as electronic collimation. However, there may be a finite difference in the detection time of both photons due to different photon travel times and different signal processing times. Thus, there must be a finite timing window (typically ~ 2 to 12 ns) in order to account for these time differences. However, such a timing window would allow photons produced from uncorrelated annihilation events to also produce coincidence events, called random events. Such events as well as events arising from scattered photons contribute to image noise. Different techniques, including setting an energy window around 511 KeV and modeling the number of random and scatter coincident events, are used to reduce the perturbing effect of such events.[33] To image moving lesions, which if conventionally imaged would result in a larger "blurred" avid region with lower signal-to-background ratios, modern PET scanners are capable of binning the detected signal into amplitude/phase bins of a patient's breathing trace. This allows for visualization of lesion motion and also allows for accumulation of the PET lesion signals from the different phases into a single phase.

Many modern scanners now possess scintillators and electronics fast and stable enough to include a technique known as time-of-flight (TOF), which works by exploiting the ability to resolve small differences in the arrival times of two valid annihilation photons to further isolate where the annihilation event occurred along a given line of response. TOF imaging increases the signal-to-noise (SNR) ratio allowing shorter scan times for the same image quality or less noisy images for the same scan time. The extent of improvement depends on the size of the patient, with larger cross-section patients deriving greater benefit compared to smaller cross-section patients. This can allow for administration of lower activities to patients (and thus lower radiation dose to the patient) or shorter acquisition times, or improved imaging of faster decaying positron emitting radiopharmaceuticals such as ^{15}O.

Resolution modeling[34–36] reconstruction has been added to PET/CT systems in the recent past. Resolution modeling essentially deconvolves the blurring of a point source (point spread function) during image reconstruction. Thus, images with higher and more uniform spatial resolution can be generated. Although this may result in increased lesion detectability, its quantitative properties are still under debate because resolution modeling is also known to introduce edge "ringing" or Gibbs-type artifacts.[36,37] In cases where quantification is based on maximum Standardized Uptake Value (SUV_{max}), use of resolution modeling may result in large upward biases under clinically relevant count statistics.[38] We envision that more sophisticated implementations of this method will be able to mitigate Gibbs artifacts while still

enhancing spatial resolution in the reconstructed images. Finally, the impact of using resolution modeling on tumor delineation accuracy and precision still needs to be assessed.

In 2004, PET/CT systems accounted for approximately 65% of all PET systems sold[39] and, today, no major manufacturer offers a PET system without a combined CT (standalone PET systems in the United States have, for the most part, disappeared from use). Recently, hybrid PET/MRI has been clinically available and may also contribute to target volume delineation and better RT treatment planning.[40,41] One study[42] seems to suggest that PET/MR and PET/CT performed equivalently for cancer assessments when MRI is used only for anatomic information, that is, not considering information provided by multiparametric MRI. It is yet early to clinically compare PET/CT vs PET/MR systems since PET/MR techniques in oncology are evolving.

Future developments in PET include continuous bed motion imaging[43,44] and so-called "Total-body" imaging using very long axial field of view (FOV) scanners, potentially increasing the sensitivity approximately 40-fold in going from a 20-cm axial FOV to 200-cm axial FOV.[45]

2.A.2. PET only and PET/CT clinical RT applications

Integrated PET/CT systems have been shown to improve lesion detectability over PET-alone systems,[46] and, additionally, advantages of a PET/CT system include patient convenience and higher clinical throughput because CT images are typically acquired for RT planning purposes.

Treatment planning using a separate PET scan relies on accurate image registration with a CT dataset, which can be difficult to ensure because of the uncertainties associated with matching landmarks between functional and anatomical datasets. It is in such scenarios that PET/CT offers several advantages. First, with no patient motion or repositioning between scans, the two datasets are inherently registered. Second, with the addition of a laser positioning package and flattop couch, the CT can be used as a CT simulator and images can be directly imported into the treatment planning software. Third, the CT scan provides information for PET attenuation correction. In the event that a separate CT-sim is used to acquire the CT for planning purposes (e.g., CT-sim acquired in RT Department, PET/CT acquired in Radiology Department), the generally high accuracy associated with registering the CT dataset from CT-sim to the CT dataset from PET/CT (assuming that both systems have a flattop couch and the same patient immobilization is used) permits the accurate transfer of information from the PET dataset to the planning CT dataset.

Given the differences in imaging capabilities, it is natural that PET and CT technologies have been combined to take advantage of the complementary information each imaging modality offers. CT allows the direct measurement of electron densities essential for RT dose calculations as well as PET attenuation correction. Coupled with simulation technology, a CT scan is an essential part of modern RT. Manufacturers have incorporated (or, are in the process of incorporating) several features in the CT portion of PET/CT units to allow for full RT simulation capabilities:

1. Larger bore CT units allow the patient to be imaged together with the patient's immobilization devices in place, such as stereotactic frames, body conformed cradles, and breast boards. This minimizes the differences in patient positioning between the planning CT and the treatment position, helping improve patient treatment setup.
2. CT-simulation isocenter placement.
3. Lasers to mark the CT-simulation isocenter on patient's skin/immobilization device.
4. Respiratory gating

The addition of these features is essentially analogous to the changes made to diagnostic Radiology CT scanners to enable RT CT-simulation. Furthermore, all major manufacturers now offer software that automatically displays PET and CT information either side by side, or fused to allow the overlay of the functional PET information on the CT dataset. The latter technique allows radiation oncologists and nuclear medicine physicians to distinguish between increased uptake from tumor vs inflammation or brown fat, for example, based on anatomical feature matching between the CT and PET images.

2.A.3. PET tracers

The most common radiotracer used in PET is [^{18}F]FDG (physical half-life: 109.7 min, biological half-life: 6–10 h). FDG is a glucose analog where the hydroxyl (OH) group on the second carbon in glucose is replaced with ^{18}F. Normal glucose undergoes several metabolic steps and can be converted to glycogen, lactate (anaerobic metabolism), pyruvate (which can then enter the citrate cycle), or enters the pentose monophosphate pathway. FDG, however, does not undergo further metabolism after its first phosphorylation stage to FDG-6-PO4.[47] FDG-6-PO4 cannot easily pass across cell membranes and for practical purposes, remains trapped in the cell. FDG uptake and retention thus reflect expression and activity of transmembrane glucose receptors and the first step of glucose metabolism. Since many cancerous cells are known to exhibit increased glucose demands, [^{18}F]FDG is a versatile radiotracer.

Aside from [^{18}F]FDG, there remains limited commercial availability of positron emitting radiopharmaceuticals. As of this writing, ten PET radiotracers have been approved for clinical use by the US Food and Drug Administration (US FDA). Not including [^{18}F]FDG, they are: [^{11}C]Choline (prostate cancer recurrence imaging); [^{18}F]Florbetaben (brain plaque density measurement); [^{18}F]Florbetapir (brain plaque density measurement); [^{18}F]Fluciclovine (prostate cancer recurrence imaging); [^{18}F]Flutemetamol (brain plaque density measurement); [^{18}F]Sodium Fluoride (altered osteopathic activity imaging); [^{68}Ga]Dotatate (localization of somatostatin receptor positive neuroendocrine tumors); [^{13}N]Ammonia (myocardial imaging); [^{82}Rb]Chloride (myocardial imaging).

2.B. [^{18}F]FDG-PET quantification using the Standardized Uptake Value (SUV)

[^{18}F]FDG-PET has the potential to be used as a quantitative imaging modality if confounding factors are accounted for. Two of the largest sources of variation are the amount of injected [^{18}F]FDG and the size of the patient. To approximately normalize for these two effects, the standardized uptake value (SUV) is a measure of uptake defined as the tissue activity per unit volume normalized by the decay-corrected injected activity and body weight. The advantage of the SUV metric is the ability to compare uptake intensities between patient images. The most common approach is to normalize activity concentration using patient body weight (BW):

$$SUV_{BW} = \frac{Activity\left[\frac{Bq}{ml}\right]}{\left(\frac{InjectedDose[Bq]}{BodyWeight[g]}\right)}\left(\frac{g}{ml}\right) \quad (1)$$

where the activities in the numerator and denominator are calculated for a common time point, typically the start of the PET scan.

However, using a patient's weight to normalize the injected activity can confound the SUV_{BW} values for obese patients, since adipose tissue takes up [^{18}F]FDG far less avidly than many other tissues. Alternate normalization methods, including using the body surface area,[48] or lean body mass[49] to make SUV independent of adipose tissue, have been proposed but are still not commonly used clinically. Other issues such as the influence of the post-injection time when the SUV measurement is taken,[50–52] plasma glucose levels,[53,54] object size and the partial volume effect, region of interest placement,[55] PET scanner and reconstruction parameters,[56–58] and patient motion[59] must be accounted for if the SUV is to be used as a metric for comparison intrapatient or interpatients. SUV has been shown to strongly depend on image noise and image resolution[57,60] since it is computed on a pixel-basis (as opposed to metrics that are, for example, averaged over a volume), which may hamper the ability to compare SUVs between images acquired on different scanner makes. For quantitative analysis, it is important that the patient follows a strict preparation procedure (an example of such a procedure is provided in Appendix S2 — discussed in Section 3 (recommendations)). Quantitative analysis can also be hampered by the presence of PET artifacts because of the presence of metal implants and dental hardware whose attenuation effects are not properly accounted for in the attenuation corrected image. In such cases, radiologists may choose to qualitatively look at the nonattenuation corrected image for guidance.

Several measures of SUV are commonly used to quantify tumor metabolism: SUV_{mean} (mean SUV value within the defined tumor boundary), SUV_{max} (maximum SUV value within the defined tumor boundary), SUV_{peak} (average SUV value within a 1 cc region of interest positioned within the defined tumor boundary so as to achieve the maximum average value), TLG (total lesion glycolysis — product of SUV_{mean} and the volume within the defined tumor boundary). In 2008, the Quantitative Imaging Biomarkers Alliance (QIBA) formed by the Radiological Society of North America (RSNA) suggested that averaging over a larger regions of interest (e.g., SUV_{peak}) may be more robustly reproducible than SUV_{max} and recommended a 1.2-cm diameter sphere (or 1 cm^3 volume) region of interest.[61]

SUV has been used in RT to differentiate malignant from benign tumors, for example, in a retrospective analysis, SUV = 2.5 in mediastinal tumor staging was deduced as a threshold above which a lesion is deemed malignant[62]; overall survival was significantly longer in a group of 176 non-small cell lung cancer patients undergoing surgery with $SUV_{max} \leq 15$ than those with $SUV_{max} > 15$.[63] Further correlations between increased [^{18}F]FDG uptake measured by SUV and poorer prognosis have been reported for many cancers, including breast cancer,[64] metastatic prostate cancer (prospective study),[65] sarcomas (retrospective analysis),[66] and Hürthle Cell thyroid cancer (retrospective analysis).[67] However, one must be cautious when using an SUV cutoff value. The 2006–2007 IAEA expert report[68] notes: "... SUV measurement can be unreliable and can suffer from problems with accuracy and reproducibility. By itself, an SUV cutoff may be inadequate for RT planning."

2.C. Utilization of [^{18}F]FDG-PET in RT

2.C.1. Staging

PET staging is typically carried out by Nuclear Medicine physicians, with appropriate input from RT physicians on the patient's overall presentation. The TNM (T = tumor size, N = nodal involvement, M = metastatic spread) system is the current clinical standard for the staging of many cancers. In this system, a patient's illness is staged based on tumor size and spread characteristics unique to the particular disease site (e.g., in lung cancer, T2aN2M1 indicates: a tumor greater than 3 cm but <5 cm in greatest dimension, metastasis in ipsilateral mediastinal and/or subcarinal lymph nodes, distant metastasis). Staging is important for several reasons, the most important being that the stage of the disease is a strong prognostic indicator and therefore affects patient management. Typically, a patient presenting with symptoms will undergo one or more diagnostic tests to determine the stage of the disease. PET has been shown to aid in more accurately staging individual patients.[69] PET has been used to improve the diagnostic ability, staging accuracy, and treatment management for a variety of cancers such as head and neck, colorectal, and malignant melanoma. Specifically, the use of PET has been shown to change patient management in several cancers with treatment intent being changed from curative to palliative[70–72] or vice versa.

2.C.2. Segmentation

An important utility of [^{18}F]FDG-PET imaging in RT is accurate segmentation of the PET avid region, so it can be included in the target. PET typically informs segmentation of the gross tumor volume (GTV: gross palpable/visible/demonstrable malignant growth[73]), which is further expanded to

create a clinical target volume (CTV: GTV and additional surrounding subclinical microscopic malignant disease, which has to be eliminated[73]). PET-guidance has clearly been shown to influence segmentation by changing manual tumor contours drawn only with CT guidance.[70,74,75] The consequence of not including some portion of the PET avid region is to underdose that region, potentially leading to lower tumor control and higher risk of recurrence.

Segmenting PET avid regions is challenging because of biological, technical, and physical factors that affect the relation between the biological uptake of FDG and PET image values, and thereby PET segmentation.[76,77] PET detectors have an inherent resolution limitation, on the order of several millimeters, implying that the boundaries of the high uptake region will appear blurred in the image. If the high uptake region is very small, this blurring effect will diminish the overall intensity, making it more difficult to distinguish from the background. In addition to the blurring effect, image noise is always present. Motion of the tumor, as in lung or liver, can blur tumor boundaries and lower SUV. Uptake intensity in tumors near the bladder may be altered due to reconstruction artifacts created by the presence of high urine intensity in the bladder. The time point at which the image is acquired after injection can influence the appearance of the high uptake region relative to background.[50] Imaging soon after injection could be compromised by insufficient radiotracer extravasation.

Manual segmentation of the PET avid region for RT is dependent on individual preference and level of experience. Typically, the CT acquired at the time of PET (PET/CT imaging) is used as an anatomical reference image to guide the PET segmentation. Modern RT planning systems are capable of superimposing the PET image on the CT image. The radiation oncologist then adjusts the PET window/level and manually outlines the FDG-avid region, simultaneously visualizing the CT image. The PET window/level adjustment is subjective and hence can be highly variable between institutions and even between radiation oncologists in the same institution. Some radiation oncologists use guidelines previously provided from phantom experiments or patient imaging. Phantom experiments have suggested setting the lower window level to various percentages of the maximum intensity in the FDG-avid region and using this threshold for segmentation, for example, 42%,[78] 41%.[79] For lung cancer patient imaging, a prospective study[80] has suggested an SUV of 2.5 as a threshold for segmentation. However, use of such threshold levels is not reliable,[81] as described earlier. The 2006–2007 IAEA expert report[68] notes that "By itself, an SUV cutoff may be inadequate for RT planning." This report was updated in 2014[82] with the reccomendation that "... outside of a clinical trial context, target volumes generated with the use of PET should be delineated using visual interpretation alone or should be visually edited following any automated target volume delineation."

As a consequence of the subjective nature of manual segmentation, automatic segmentation methods have been developed with the aim of producing unbiased or at least reproducible estimates of the lesion boundary based on phantom studies or mimicking expert consensus in human cases.[77] These methods are typically developed in phantom experiments where several inserts (usually spherical) filled with [^{18}F]FDG are placed within a large container filled with some background concentration. These experiments are typically carried out with the ratios of insert-to-background concentrations varied over ranges seen in human scans. Since the ground truth, that is, insert volumes, is known, automatic segmentation methods can be developed and tested on them. Threshold-based segmentation,[78,83–85] gradient-based segmentation,[86,87] region-growing segmentation,[88] consensus segmentation,[89] and combined PET/CT or PET/MR segmentation[90,91] are only a few examples of automatic segmentation methods. The important point to note with automatic segmentation methods is that they have not been extensively validated in animals or humans. It is our understanding that there is not a universally accurate automatic segmentation method at the present time. The reader is referred to the report of the AAPM Task Group 211 (TG-211: Classification, Advantages, and Limitations of the Auto-Segmentation Approaches for PET) for an extensive review of segmentation methods and guidelines.[77]

2.C.3. Image registration

Positron emission tomography imaging information is transferred via rigid and/or deformable image registration onto the treatment planning CT. This is generally not an issue when the treatment planning CT and PET images are acquired in the same session on a PET/CT system, since images from the two modalities are inherently registered to each other (in the absence of motion). However, if the planning CT dataset and PET/CT dataset are acquired on different systems, transfer of PET information to the planning CT dataset occurs via registration between the CT dataset from PET/CT and planning CT dataset. In this case, CT-CT rigid registration can usually be achieved with high accuracy, assuming: a short time interval between the acquisition of the planning CT and PET/CT datasets (i.e., insignificant changes in patient anatomy), flattop tables on both systems, and the same patient immobilization on both systems.

Accurate image registration is crucially important when used for treatment assessment from two or more longitudinally acquired datasets in the same patient (e.g., before treatment and after/during treatment), where anatomic changes can be significant. In this case, volumes from the initial dataset are required to be translated to subsequently acquired datasets to enable quantification of the PET changes. Typically, this is achieved by the registration of the initial CT images to the subsequent CT images. Volumes can then be transferred from the initial CT images to subsequent CT images and then to the automatically coregistered PET images.

In RT, PET image registration is used for the following purposes among others: (a) better tumor target definition[92]; (b) propagation of contours from one image set to another[93];

(c) adaptive therapy planning/dose painting to selectively increase dose to more PET-avid target regions[94–96]; and (d) incorporation of respiratory-gated PET information in treatment planning.[97–99] The reader is referred to AAPM Task Group 132 (TG-132: Use of Image Registration and Fusion Algorithms and Techniques in Radiotherapy),[100] which deals with the topic of image registration in RT.

Image registration is divided into rigid and deformable registrations. The former has been used in RT for over two decades, whereas the latter is still under intensive investigation and should be used with caution in clinical practice. Many registration techniques exist in the literature: landmark-based, surface-based, and intensity-based (e.g., squared error, cross correlation, mutual information) registrations. Depending on the mechanism used to model the deformation, deformable registration methods can usually be categorized into elastic models,[101–103] viscous fluid models,[104] diffusion models (demons),[105] optical flow models,[106–108] finite element models (FEM, or biomechanical model),[102,109] radial basis function (RBF) models such as basis spline model,[110–112] thin plate spline models,[113–116] etc.

Despite years of intensive research, a universally accepted deformable registration model still does not exist. The inherent complexity of the problem and general lack of ground truth information on the deformation vector field in test cases makes it difficult to validate these models. The demand for deformable registration models will increase in the future as more molecular imaging modalities are developed and start being used in clinics or small animal imaging laboratory. It is thus critically important to develop more robust image registration techniques to maximally utilize the information provided by state-of-the-art molecular imaging modalities.

2.C.4. Respiratory gating

Respiration-induced motion within the thoracic and abdominal cavities results in lesion motion, thereby spreading the radiotracer activity over an increased volume, distorting apparent tumor shape and location, and reducing both signal and signal-to-noise ratio levels. In light of the millimeter-level precision of modern conformal and intensity-modulated treatment planning, these artifacts are particularly worrisome for small lesions located in the lung, liver, or pancreas. Gating the data acquisition either prospectively or retrospectively is a solution, effectively limiting the image analysis to a single phase of the respiratory cycle. A major disadvantage of both retrospectively and prospectively gated PET is that, since only a fraction of the scan is used during each cycle, the overall scan time must be proportionally lengthened to obtain signal levels characteristic of a motionless lesion. This increased scan time raises practical difficulties related to patient discomfort and immobilization. Increased scan time also results in lower radioactivity (and hence lower signal) at later time points during the scan. However, one should also note that, with increased scan time, while overall signal is decreased, contrast is increased because of radiopharmaceutical clearing from the blood stream.

Positron emission tomography/computed tomography units with respiratory-gated capability are increasingly being employed, where the PET signal is binned based on amplitude/phase of the breathing trace. Amplitude and phase binning essentially either divide the amplitude range or temporal range, respectively, into intervals, following which images from different axial slices corresponding to the same interval are assembled into full 3D datasets. The PET datasets corresponding to each individual interval or bin are noisier because of the lower counts per bin. The use of internal target volumes (ITVs) defined from respiratory-gated PET/CT ITVs from amplitude binning has been shown to be larger and more accurate than those from phase binning.[117] Amplitude and phase binning are achieved by subdividing a respiratory signal that is typically obtained from external hardware attached to the patient.[118] However, the respiratory signal may also be generated using a data-driven approach, from motion information contained in the PET/CT data.[119,120] Yet another approach is to acquire data only in a single bin, corresponding to either end exhale or deep inspiration breath-hold.[118]

In a research context, several investigations have looked at deforming and accumulating the PET signals from different bins into one bin (e.g., end exhale) using deformable registration. A caveat is that the accumulated PET image could have large variability based on the type of deformable registration algorithm employed. Dynamic PET, wherein time-stamped PET data are captured in list mode or sinogram formats, may be used for applications such as kinetic analysis, reconstruction algorithm development, and motion management. These applications, however, are primarily research-related and not used yet for clinical patient assessment in oncology.

2.C.5. Treatment planning

[^{18}F]FDG-PET is typically used in RT planning to guide segmentation of PET-avid target regions (see Section 2.3.2). These segmented volumes are then included as part of the larger target region. The RT prescription usually takes the larger planning target volume (gross tumor volume plus margin to account for microscopic disease spread plus margin for setup error) up to some primary dose level and then boosts the gross tumor volume (including high uptake regions) to a higher dose. The primary and boost doses are typically planned for spatially homogeneous delivery to their respective target regions.

Of late, there has been increasing clinical interest in delivering nonhomogeneous dose to the target based on [^{18}F]FDG-PET uptake, with the aim of improving local control.[121,122] Broadly, the idea is to either selectively increase dose to FDG-avid subvolumes within the target (subvolume boosting), or tailor the dose to FDG-uptake on a voxel-by-voxel (dose painting by numbers).[121] This approach has been shown to be technically feasible in the past, where high uptake regions are either uniformly taken to a higher dose or have a more tailored pattern with higher doses to higher voxel

intensities.[123–126] However, PET volumes can change during the course of radiation treatment,[127] implying that a plan generated on the PET image prior to RT may be less relevant throughout the course of RT. A study of patients with non-small cell lung cancer revealed that, while the volumes themselves may become smaller, areas of low and high FDG uptake overlapped reasonably well on serial images acquired at various time points during the course of RT.[128] This suggests that a plan generated with the initial FDG image may remain relevant through the course of therapy, but this has yet to be comprehensively validated. A confounding effect is radiation-induced inflammation, leading to increased tumor PET uptake on images acquired during the course of RT, making it difficult to assess metabolic tumor response.

Some clinical studies have instituted the approach of tailoring dose to high FDG uptake regions. An example is a multicenter randomized Phase 2 trial for Stage 2–3 non-small cell lung cancer,[129,130] with the primary endpoint of local progression-free survival at 1 y. This trial closed accrual in November 2017. As of this writing, results of the trial are forthcoming.

2.C.6. Therapy response assessment

[^{18}F]FDG-PET can be used to assess response to RT with or without chemotherapy. Response assessment is typically based on images acquired at one or more time points: pre-therapy or post-therapy; pre-therapy vs post-therapy; pre-therapy vs intra-therapy. The reader is recommended to extensive literature reviews on response assessment for head-and-neck cancer,[131–134] esophageal cancer,[134–136] lung cancer,[134,137,138] and uterine/cervix cancer.[139] These reviews cover response assessment based on image metrics extracted from segmented tumor volumes in the images, for example, maximum SUV, mean SUV, metabolic tumor volume (tumor volume above some SUV threshold), total lesion glycolysis (integral of SUV in the metabolic tumor volume), and, more recently, texture features. Both pre-therapy image metrics and the comparison of pre-therapy to intra-therapy (preferably at some early time point during RT) image metrics seek to prognostically separate responders from nonresponders with a view to potentially altering the therapy regimen for nonresponders. The comparison of pre-therapy vs post-therapy image metrics seeks to determine the effectiveness of the entire course of therapy and also determine/predict patients who are likely to have disease recurrence.

3. RECOMMENDATIONS FOR CONSISTENCY OF [^{18}F]FDG-PET USAGE IN RT

All recommendations made in this section are intended to apply to PET or PET/CT systems used to acquire scans on RT patients, irrespective of whether these systems are located within or outside a RT Department.

In the event of failure of a test (or tests) outlined below, it is expected that a QMP, or individuals working under the supervision of a QMP, will work with the PET/CT scanner vendor to resolve the issue.

3.A. Acceptance testing and quality assurance

Many parameters affect the quality and accuracy of a PET/CT image such as sensitivity, linearity, uniformity, spatial resolution, contrast, noise, attenuation, and random and scatter events subtraction accuracy, calibration, partial volume effects, etc. Several protocols have been established that assess scanner performance and recommend quality assurance (QA) procedures, test frequencies, and action levels. For example, the National Electrical Manufacturers Association [NEMA; PET-related activities are conducted by a suborganization called the Medical Imaging Technology Alliance (MITA)],[140] SNMMI (Society of Nuclear Medicine and Molecular Imaging) clinical trials network scanner validation program,[141] the ACR (American College of Radiology) Technical Standards for PET/CT,[142] and the EARL/EANM (European Association of Nuclear Medicine/EANM Research Ltd) [^{18}F]FDG PET/CT accreditation program[143] in Europe all have recommendations to evaluate PET system performance. AAPM task group 126 (TG-126: PET/CT Acceptance Testing and Quality Assurance) is charged to establish acceptance testing and routine QA of PET/CT scanners, with recommendations expected by the time of this publication. The IAEA published a detailed guide of QA for PET & PET/CT[144] that also describes QA procedures for PET and PET/CT systems and their recommended frequency. In 2008, the Radiological Society of North America (RSNA) sponsored the formation of the Quantitative Imaging Biomarkers Alliance (QIBA), which includes a program in [^{18}F]FDG PET/CT imaging. The main role of the QIBA Technical Committee is to produce a new type of document called a "Profile" that provides a consensus of the measurement accuracy of a quantitative imaging biomarker for a specific use, and the requirements and procedures needed to achieve this level of measurement accuracy. In the case of the [^{18}F]FDG PET/CT Profile, the "Claim" states:

> *If Profile criteria are met, then tumor glycolytic activity as reflected by the maximum standardized uptake value (SUVmax) should be measurable from FDG-PET/CT with a within-subject coefficient of variation of 10%–12%.*

Note that within-subject coefficient refers to measurement repeatability. In the creation of the initial QIBA [^{18}F]FDG-PET/CT Profile, there were over 100 participants. Review and feedback from several dozen individuals and organizations were incorporated in the final version, which was released in December 2013.[61]

Collectively, these recommendations are necessary to ensure the accuracy and reproducibility of quantitative PET and PET/CT measurements. This is particularly important in longitudinal studies as well as studies across multiple centers, given the differences in design and performance of these systems. The impact of design/performance differences was demonstrated by Bergman,[145] who followed the NEMA

protocol to assess image quality variation between 15 scanners using the International Electrotechnical Commission (IEC) body phantom containing six spheres of varying diameter and activity concentrations relative to background. They found considerable differences in image quality, calling into question the clinical interpretation of images and measurement of quantitative indices such as the standardized uptake value.

Ultimately, the purchasing specifications sent to a vendor in the Request for Proposals (RFP) and QA appropriate for PET/CT in RT are dependent on how the system is to be utilized. For example, in RT, Xing[146] described QA directed toward PET/CT where, in addition to general system performance assessment and QA, issues surrounding data transfer, consistency of SUV, multimodality image fusion, system integration, and respiratory motion management were considered. The frequency and action levels of system testing have been investigated for many systems,[147–149] with an emerging philosophical shift being introduced by Task Group 100 of the AAPM (TG-100: Method for Evaluating QA needs in RT).[150] The TG-100 approach utilizes "Failure Modes and Effects Analysis" (FMEA) to better implement QA programs based on institutional procedures.

3.A.1. Acceptance testing

Acceptance testing procedures should always be performed by a QMP, or individuals working under the supervision of a QMP, to verify that the manufacturer has delivered and installed a product that meets all the agreed upon purchase specifications.

The QMP and individuals working under the supervision of the QMP should detail all the desired specifications of the PET/CT scanner to be utilized in RT as part of the RFP sent out to the vendors soliciting bids prior to purchase. Along with required specifications, the RFP should define the procedures to be followed during acceptance testing. The acceptance testing procedures for the CT portion of the PET/CT machine should at least incorporate the quality assurance recommendations of AAPM Task Group 66.[151] The PET portion of the PET/CT acceptance testing procedure should include the performance measures from NEMA NU 2-2012 (http://www.nema.org/stds/nu2.cfm) with manufacturer specifications for passing criteria. NEMA NU 2-2012 uses three phantoms to measure spatial resolution, sensitivity, scatter fraction, count rate performance, count rate correction accuracy, and image quality. The recommended annual QA procedure and monthly QA procedure (see subsections below) should also be included in the acceptance testing procedure. The annual QA procedure ensures that absolute SUV values, SUV ratios, and resolution tests meet required standards as described by ACR standards or EARL accreditation criteria (EU), and sets baselines to be compared against during subsequent QA tests. These standards assure accurate scanner calibration and consistent and harmonized (quantitative) performance of the PET/CT systems. The monthly QA procedure also checks the registration of PET and CT images, using the cylinders and rods (ACR) and/or spheres, lung insert, and rods (EARL) as landmarks. Offsets or skews will indicate the need for alignment corrections.

Please note that future recommendations from TG-126 could supplement (but not obviate) the recommendations of this task group report.

3.A.2. Annual QA

It is recommended that PET or PET/CT systems be compliant with the specifications of the tests detailed in the ACR Nuclear Medicine & PET accreditation program (https:///www.acraccreditation.org) or the EARL [^{18}F] FDG PET/CT accreditation program in Europe. While it is recommended that compliance be demonstrated via accreditation, the tests may alternatively be internally validated by a QMP or individuals working under the supervision of a QMP.

A portion of the ACR procedure, that is, pass/fail criteria for SUV values (Table 1 with the exception of the last three rows), is recommended to be used as part of the annual QA, with additional checks for resolvability and PET/CT image alignment (last three rows of Table 1). The ACR tests for SUV values consist of scanning an ACR approved PET phantom (Data Spectrum's ACR flangeless PET phantom (www.spect.com)) and entering the results in Table 1 to determine pass/failure. The ACR-approved PET phantom is a 20.4-cm internal diameter cylindrical phantom with end plates. The phantom consists of two sections, a bottom section with a set of acrylic rods for resolution determination, and a top section with hollow cylinders and a bone equivalent Teflon rod. The phantom is filled with background activity water, and the hollow cylinders are either filled with higher activity water or water with no activity, for absolute SUV and SUV ratio determination. It is recommended to follow the procedure as detailed in the PET accreditation document (PET Phantom Instructions for Evaluation of PET Image Quality; ACR Nuclear Medicine Accreditation Program; PET Module) obtainable from the ACR accreditation site (https:///www.acraccreditation.org).

Table I documents the results and pass/fail checks ("hot"/"cold" refers to high/low radioactivity levels). In keeping with the QIBA claim,[61] it is recommended that deviations larger than 10% from the baseline values (acquired at the time of acceptance) for the mean SUV of the background, maximum SUV of the 25 mm cylinder, and ratio of maximum SUVs of the 16–25 mm cylinders be flagged as "fail," requiring further investigation by the vendor service team. The last three rows of Table 1 check for resolvability and PET/CT alignment. Note that the measurements in Table I are not meant to indicate comprehensive QA of the PET scanner (as will result from TG-126, mentioned earlier), but rather to document a minimum level of acceptable imaging reproducibility. Details on the EARL procedures and performance specifications can be found at http://earl.eanm.org/cms/website.php?xml:id=/en/projects/fdg_pet_ct_accreditation.htm.

TABLE I. Phantom Scan Parameters (data spectrum's ACR flangeless PET phantom) and results.

I. Scan Parameters	
Transmission Scan Processing	☐ CT KV _____ mAs_____ pitch_____ metal/high density artifact correction_____ truncation correction_____ ☐ Segmentation ☐ Segmentation+emission subtraction ☐ Other_____
PET scan parameters	Number of bed positions _____ Time/bed position (min) _____ bed overlap (# slices/mm/%)_____ Emission start time (hh:mm:ss) _____ Activity at emission start time (Bq) _____ Emission mode ☐ 2D ☐ 3D Matrix size _____ Zoom/FOV (mm)_____
Reconstruction method (FBP, OSEM, etc.)	☐ FBP ☐ OSEM ☐ RAMLA ☐ other If OSEM: iterations _____ subsets _____ PSF/resolution modeling _____ TOF (yes/no)_____ Pixel size _____
Processing Filter	Filter type _____ Setting _____
Slice thickness (mm)	
II. Phantom Scan Results (according to ACR standards)	
Mean SUV of background (central 6 cm diameter region on axial slice) (slice at longitudinal center of cylinders)	_____ Pass/Fail (Pass: SUV 0.85 – 1.15) Baseline value _____ % deviation _____ (Pass: < 10%)
Max SUV of 25 mm cylinder (slice at longitudinal center of cylinders)	_____ Pass/Fail (Pass: SUV > 1.8 to < 2.8) Baseline value _____ % deviation _____ (Pass: < 10%)
Ratio of max SUVs 16mm/25mm (slice at longitudinal center of cylinders)	_____Pass/Fail (Pass: ratio > 0.7) Baseline value _____ % deviation _____ (Pass: < 10%)
PET/CT alignment check: Visually examine alignment between CT and PET images for the cylinders (4 "hot", 1 "cold", 1 empty, 1 Teflon rod). Manually align the PET and CT images using visual inspection and report the alignment distance along X, Y, and Z direction. Limits: +/- 2mm in any direction.	_____Pass/Fail (Pass: within ±2 mm in any direction[62].)

These results are also recommended to be included in publications, as elaborated later.

The annual QA procedure for the CT portion of the PET/CT machine should at least incorporate the recommendations of AAPM Task Group 66.[151] In brief, annual QA of the CT includes CT Dose Index (CTDI) measurement, table indexing and position, gantry tilt accuracy, scan localization, radiation/sensitivity profile width, CT number accuracy, electron

density to CT number conversion, spatial resolution, contrast resolution, and field uniformity.

The nuclear medicine portion of the annual QA should be performed by a QMP or individuals working under the supervision of a QMP; the corresponding CT portion should be conducted by the Radiation Oncology Quality Assurance Committee as recommended in AAPM Task Group 66[151].

3.A.3. Monthly QA and Daily QA

Monthly QA of the CT portion of the PET/CT machine should comply with the recommendations of TG-66[151] and includes orientation of the gantry lasers with respect to the imaging plane, spacing of lateral wall lasers with respect to lateral gantry lasers and scanning plane, orientation of wall lasers with respect to the imaging plane, orientation of ceiling laser with respect to the imaging plane, orientation of CT scanner tabletop with respect to the imaging plane, table vertical and longitudinal motion, table sag, CT number accuracy, in-plane spatial integrity, and field uniformity. The monthly QA for PET (Appendix S1) is not intended as comprehensive testing, but rather to provide constancy checks on uniformity, quantification, scatter and randoms correction, spatial resolution, and PET/CT alignment. The nuclear medicine portion of the monthly QA should be performed by a QMP or individuals working under the supervision of a QMP; the corresponding CT portion should be conducted by individuals as recommended in AAPM Task Group 66.[151]

Daily QA should be performed in accordance with manufacturer specifications and local/state regulations.

3.B. Scanning protocol

There are several consensus protocols describing [^{18}F] FDG-PET/CT scanning protocols for diagnostic imaging[30,76,152] and quantitative SUV imaging.[61] However, this committee is not aware of consensus protocols for [^{18}F]FDG-PET/CT imaging specifically for RT simulation and planning. While many scanning requirements are common to diagnostic imaging, quantitative imaging, and RT planning protocols, it is imperative as a medical physics community to identify and standardize the unique elements of [^{18}F]FDG-PET/CT scans for RT planning.

A patient workup for PET scanning of RT patients takes about 2 h. These are the typical steps taken during those 2 h:

1. Prior to arrival patient is instructed to fast a minimum of 4 h.
2. Patient arrives.
3. Height and weight measured.
4. Serum glucose level measured (may need to reschedule patient if blood glucose level is greater than some set value, e.g., 150 mg/dL).
5. Radiopharmacy notified of patient arrival.
6. Patient radiopharmaceutical prepared in the radiopharmacy (activity and assay time noted).
7. Immobilization device fabricated in PET/CT (schedule permitting), or fabricated in RT CT simulator for transport to PET/CT.
8. Patient radiopharmaceutical transported to injection area.
9. Patient injected and time of injection noted. Residual activity and associated assay time noted.
10. Patient waits 55–75 min (target time 60 min) in a quiet shielded room. In many facilities, the patient drinks (diluted positive or negative) oral contrast for contrast-enhanced CT imaging, if applicable. Note that the schedule should be adjusted for certain oral contrast agents that need to be taken 2–4 h prior to scanning.
11. Technologist arrives and requests the patient to go to the bathroom to empty bladder.
12. Immediately before proceeding to the scanner room, the patient may drink another cup of oral contrast if this is part of the protocol.
13. Technologist mounts flat carbon fiber indexable table for RT simulation and planning in place of cushioned diagnostic couch.
14. Patient goes to the imaging room.
15. Setup on the table, indexing of immobilization, and patient alignment to external wall-mounted lasers — ~15 min.
16. Patient info entered into the system.
17. Scout view — 1 min.
18. CT scan — 2 min (low dose for attenuation correction if appropriate).
19. PET scan — this depends on the local protocol, field of view, and number of bed positions. Each bed position should be on "3D mode" if feasible and take approximately 2–4 min/bed position.
20. Diagnostic CT with/without intravenous contrast.

RT-specific protocols for PET are required due to the unique challenges that arise when integrating the functional information PET provides into the diagnostic, treatment planning, and response monitoring phases of a patient's care. While diagnostic PET is used predominantly for the diagnosis and staging of disease, it can be used to define target volumes and assess treatment efficacy. Given that there are several factors that directly affect a PET image (e.g., patient history, respiratory motion, scan duration, subject positioning, time between tracer injection and scan, reconstruction parameters),[153] standard protocols are essential for accurate and reproducible development and assessment of RT treatments. This consistency allows more accuracy in inter- and intrapatient comparisons. Stronger conclusions may also be drawn from larger multi-institutional studies if the same protocol is followed.

The following categories can influence the PET uptake distribution, and hence, controllable parameters should be as consistent as possible between different patients on the same trial and for repeated imaging in the same patient (e.g., response assessment):

- Patient parameters in the time period (hours/days) prior to administration of radiopharmaceutical: Food intake, physical activity, glucose level.
- Activity administration parameters: Radiopharmaceutical activity administered, patient weight, injection site, other drugs (muscle relaxants, pain medication, etc.).
- Patient parameters in time period immediately post administration of radiopharmaceutical: Length of time period between radiopharmaceutical administration and scanning, waiting room temperature, physical activity.
- Imaging parameters: Scanner type, attenuation correction, image acquisition time, motion correction/ respiratory gating, image processing parameters (reconstruction algorithm, filtering).
- Parameters in registration of PET images to planning CT image: Immobilization (preferably same as for RT treatment), alignment of PET to CT in a PET/CT system, alignment of planning CT from CT-sim system to CT from PET/CT system, alignment of lasers to patient marks for definition of imaging origin in RT planning system (PET/CT simulation).

The extent to which the parameters mentioned above affect the quantitative interpretation of a PET image is incompletely understood, at least for some parameters, at the present time. Consequently, it is recommended that these parameters be consistent in inter- and intrapatient scans. Table II is recommended to be used to ensure that the parameters are consistent, to the best extent possible, in an actual clinical setting (parameters in Table II are extracted in part from "ACRIN 922: Patient Preparation and FDG Administration Procedure for ACRIN FDG PET Scans" (http://www.acrin.org/Portals/0/Corelabs/ACRINPatientPrep_SOP%203-17-10.pdf), "ACRIN 923: Image Acquisition and Processing for ACRIN PET Scans" (http://www.acrin.org/Portals/0/Corelabs/ACRINImageAcq_SOP%203-17-10.pdf), and "QIBA Profile. FDG PET/CT as an Imaging Biomarker Measuring Response to Cancer Therapy[61]"). The first column lists the parameters. The second column is the template containing the parameter values (or ranges) to be used for all patients on the trial. The third column is for the actual parameter values used for a specific patient. Thus, for a clinical study (inter- and intrapatient), Table II would serve to maintain consistency of the parameters, while serving as documentation of the actual parameter values used for each patient. Table II is recommended to be used irrespective of whether the PET scans are acquired in a RT department or as part of a diagnostic procedure in a Radiology department. Table II is recommended to be used in conjunction with a PET/CT scanning protocol that is included in the institutional policies and procedures documentation to ensure internal consistency (an example is given in Appendix S2).

3.C. Reporting in literature

Most RT literature on the use of PET in clinical studies is not consistent in reporting the actual patient and scanning parameters used. Also, in many cases, not enough detail is given for the same work to be validated/replicated or continued at a different institution. The physicians (RT, Nuclear Medicine) and physicists (RT, Nuclear Medicine) constituting this task group recommend that Table III be used in publications to document details of the patient and scan parameters. Refer to Table I for details regarding Section III of the table (phantom scan parameters). Table III is a minimum list; additional parameters may be included if deemed important.

3.D. Treatment planning system [^{18}F]FDG-PET-specific requirements

Several deficiencies exist with current treatment planning systems when used in conjunction with PET and PET/CT systems. These deficiencies and recommendations for rectifying them are listed below:

1. Conversion of PET image to SUV

Currently, almost none of the treatment planning systems (TPSs) provides a tool for converting the PET pixel/intensity data to SUV. Treatment planning systems display the PET data as raw values, while all PET vendors support the display of PET images as SUV. In this regard, TPSs should, at a minimum, be user-friendly in terms of allowing the user to modify (or correct) the PET raw values to SUV through a conversion function. In addition, TPSs should have the capability of reporting the SUV histogram within a region of interest (ROI) as well as the region's maximum, minimum, mean, and peak SUVs. It is also recommended that the accuracy of the SUV calculation by the TPS be tested using the QIBA 18F-FDG-PET/CT Digital Reference Object,[154] which was specifically designed for this test.

2. Delineation of tumor using SUV cutoff/thresholding or robust segmentation algorithms, plotting of variation in PET tumor volume as a function of cutoff or threshold value, and mapping PET voxel SUV to nonuniform radiation dose prescription distributions as part of the treatment planning objectives.

Both the PET/CT (or PET) simulation programs and TPSs should have support for plotting variation in PET tumor volume as a function of cutoff/threshold value (given as absolute value, % maximum SUV value) and also using more sophisticated PET tumor segmentation algorithms (such as in Hatt et al.[155]) Additionally, it would be desirable for TPSs to have the capability to map individual PET voxel SUV to prescribed radiotherapy doses that may then be incorporated into inverse planning objective functions (e.g., dose restrictions based on SUV value).

3. Support for simultaneous fusing of (and contouring on) multiple [18F]FDG-PET image datasets (e.g., datasets from pre, during, and post-treatment)

Most TPSs support fusing of multiple datasets. However, they are not PET-specific in that they do not allow voxel-by-voxel SUV comparison and changes in maximum, mean, and peak SUV between the image sets for selected regions of

TABLE II. Patient Specific Preparation and Imaging Parameters (Template column to be filled out by Radiation Therapy Medical Physicist) Patient specific parameters should match Template parameters (grey-shaded boxes need only be filled if not in compliance with the corresponding template parameters). In the event of possible mismatch, the Radiation Therapy Medical Physicist should be consulted prior to scanning.

	Template Parameters	**Patient-Specific Parameters**
Technologist	N/A	
Patient name		
Date (month/ day/ year)	N/A	
Scanner used (relevant for institutions with multiple scanners)		
Patient weight (Kg)		
Patient height (cm)		
Exercise in 24 hrs prior to [^{18}F]FDG injection	none	
Duration of patient fasting pre-RT imaging (hours)	4 hours	
Patient voided bladder prior to injection of [^{18}F]FDG	yes	☐ no (notes) _____
Blood glucose in 1- 2 hours prior to [^{18}F]FDG injection (mg/dL)	Allowed range:	
Pre-injection activity assay (Bq)	Allowed range:	
Time of activity assay (hh:mm:ss)	N/A	
Time of injection (hh:mm:ss)	N/A	
Post injection activity assay (Bq)	N/A	
Location of injection site (use 21 gauge needle; injection should be anatomically remote to tumor site)	☐ right antecubital ☐ right wrist ☐ left antecubital ☐ left wrist ☐ right foot ☐ left foot ☐ Other _____	☐ right antecubital ☐ right wrist ☐ left antecubital ☐ left wrist ☐ right foot ☐ left foot ☐ Other _____
Waiting area parameters	Temperature (°F/°C) > 75°F/ 22°C Position: ☐ sitting _____ ☐ lying _____ Instruct to minimize talking	Temperature (°F/°C)_____ Position: ☐ sitting _____ ☐ lying _____
Water consumed following injection (> 500 ml (16 oz))	Range allowed:	
Administration of diuretic/sedative	Details_____	Details_____
Patient voided bladder immediately prior to scanning	yes	☐ no (notes) _____
Immobilization parameters (as in RT treatment, to best extent possible)	Head-neck immobilization _____ Body immobilization & knee support _____ Arm position _____	Head-neck immobilization _____ Body immobilization & knee support _____ Arm position _____

TABLE II. Continued.

Time between [^{18}F]FDG injection and start of scan	Range allowed: _____ min	_____ min
Transmission Scan	☐ low dose CT (for attenuation correction only) ☐ before PET scan ☐ after PET scan ☐ helical_____ ☐ 4D_____ Scan direction: ☐ craniocaudal ☐ caudocranial ☐ diagnostic quality planning CT ☐ before PET scan ☐ after PET scan ☐ before low dose CT ☐ after low dose CT ☐ oral contrast_____ ☐ IV contrast_____ ☐ helical_____ ☐ 4D_____ Scan direction: ☐ craniocaudal ☐ caudocranial	☐ low dose CT (for attenuation correction only) ☐ before PET scan ☐ after PET scan ☐ helical_____ ☐ 4D_____ Scan direction: ☐ craniocaudal ☐ caudocranial ☐ diagnostic quality planning CT ☐ before PET scan ☐ after PET scan ☐ before low dose CT ☐ after low dose CT ☐ oral contrast_____ ☐ IV contrast_____ ☐ helical_____ ☐ 4D_____ Scan direction: ☐ craniocaudal ☐ caudocranial
PET scan/reconstruction parameters	No. of bed positions_____ % bed overlap _____ Time/bed position (min)___ Scan range description _____ Emission mode ☐ 2D ☐ 3D Gating ☐ Phase #bins_____ ☐ Amplitude #bins_____ ☐ Other _____ ☐ FBP* ☐ OSEM* ☐RAMLA* ☐ other_____ Filter type_____ Filter Setting _____ If OSEM: iterations _____ subsets _____ Transverse smoothing _____ Axial smoothing _____ PSF*/resolution modeling in reconstruction_____ TOF* (yes/no)_____ FOV* _____ Pixel size _____	No. of bed positions _____ % bed overlap _____ Time/bed position (min)___ Scan range description _____ Emission mode ☐ 2D ☐ 3D Gating ☐ Phase #bins_____ ☐ Amplitude #bins_____ ☐ Other _____ ☐ FBP ☐ OSEM ☐RAMLA ☐ other_____ Filter type_____ Filter Setting _____ If OSEM: iterations _____ subsets _____ Transverse smoothing _____ Axial smoothing _____ PSF/resolution modeling in reconstruction_____ TOF (yes/no)_____ FOV _____ Pixel size _____

*FBP, filtered back projection; OSEM, ordered subsets expectation maximization; RAMLA, row-action maximum-likelihood algorithm; PSF, point spread function; TOF, time-of-flight; FOV, field of view.

TABLE III. Patient and scan parameters.

I. Scanner Specifications	
Scanner used - Make, Model.	
Scanner software version (list updates if patients were imaged with different versions)	
Protocol for scanner calibration	
II. Patient Specifications	
Fasting status	
Blood glucose level prior to [^{18}F]FDG injection	
Injected activity (Bq)	
Location of injection site (right/left wrist, right/left antecubital, right/left foot)	
Water consumed after [^{18}F]FDG injection (ml/oz)	
Time between [^{18}F]FDG injection and start of scan	
PET scanning and processing	2D/3D mode _____ Number of bed positions _____ Time/bed position _____ Gating _____ (phase, amplitude, # bins, etc.) Attenuation correction with CT ____ other ____ Reconstruction method: FBP__, OSEM__, RAMLA___other___ If OSEM: iterations _____, subsets _____ PSF _____, TOF (yes/no)_____, Filter _____, Slice thickness _____(cm), pixel size_____(cm)
III. Phantom Scan Parameters *Acquired from scans of Data Spectrum's ACR flangeless PET phantom*	
Mean SUV of background (central 6 cm diameter region on axial slice) (slice at longitudinal center of cylinders)	
Max SUV of 25 mm cylinder (slice at longitudinal center of cylinders)	
Ratio of max SUVs 16 mm/25 mm (slice at longitudinal center of cylinders)	

interest. These comparisons are necessary to assess treatment-induced changes during or after the course of RT.

Vendors should use the PET/CT Digital Reference Object (DRO) detailed in the QIBA profile document to validate and document the accuracy of their quantitative outputs and alignment accuracy.[61]

4. USERS WITH TPSS THAT DO NOT HAVE SOME OF THE FUNCTIONALITIES MENTIONED ABOVE SHOULD BE AWARE THAT SEVERAL NON-TPS COMMERCIAL SOFTWARE SYSTEMS ARE CAPABLE OF SOME OR ALL OF THESE FUNCTIONALITIES

4.A. Image registration

It is recommended that image registration between a planning CT image set and a PET image set that is not acquired in the same session be conducted via a CT set acquired in the same session as the PET imaging. Such a CT image set may even be acquired with low dose (typically used for attenuation correction) and then rigidly registered against the higher quality planning CT image set. Since the CT and PET image sets acquired in the same session are inherently registered in the same frame of reference, this allows registration of the PET image set to the planning CT image set. Planning CT images and PET images acquired in the same session do not require any additional registration. However, it should be validated that there is no motion between CT and PET imaging by visually checking the registration. It is recommended that the CT and PET image sets, whether acquired in the same session or not, be acquired with immobilization used during treatment.

An important assumption made in the previous paragraph is that the PET and CT images acquired in the same session are spatially registered. This may not be true if the patient

moves during the relatively longer PET acquisition. In cases where there is reason to believe that the location of the tumor and/or immobilization might allow excessive motion, acquiring a low-dose CT at the beginning and end of the session can help determine whether the registration is trustworthy.

In tumors with respiratory motion where the PET images are not gated, the PET intensity will be blurred over the motion range. In this case, registration will likely be best if the CT image set used for registration is the time-weighted average intensity projection images generated from respiratory-gated/correlated CT that incorporate similar motion blurring as the static ungated PET. The spatial variation in PET image intensity must be interpreted as the motion-convolved intensity variation, not the true intensity variation. Registration of individual respiratory-matched CT and PET images should be verified, particularly if it affects the accuracy of respiratory-gated PET attenuation correction (it is recommended that the respiratory matched 4D CT image sets be used for attenuation correction, rather than a phase-nonspecific 3D CT image set). Verification may be performed by comparing the coincidence of PET-avid regions to CT landmarks in the different phases; the coincidence should be consistent across phases, allowing for anomalous phase registrations to be flagged. PET attenuation correction may be especially affected if misregistration causes some part of the PET-avid lesion to move from a lower to higher CT density region, or vice versa, erroneously increasing/decreasing the PET intensity in the affected part of the lesion.

As mentioned earlier, deformable image registration is still an area of active research. The computed deformations can differ based on the algorithm used. Comprehensive experiments are required to validate the accuracy of these algorithms, particularly in the context of four-dimensional treatment planning and treatment response assessment. Consequently, it is recommended at the present time to employ rigid registration, not deformable registration.

4.B. Radiation dose to patients and staff

The use of PET/CT imaging is associated with increased radiation exposure to both patients and staff. The PET/CT facility should be appropriately shielded per the recommendations of AAPM Task Group 108 (TG-108: PET and PET/CT shielding requirements).[156] The typical effective dose from a combined PET/CT scan is on the order of 5–20 mSv.[157] The effective dose will depend on the site and the type of scan (gated/nongated/4D). When developing the PET/CT imaging process at an institution, consideration should not just be given to the requirements for optimal PET/CT imaging but also those for minimization of patient dose and staff exposure and following ALARA principles. Radiation exposure from patients (at patient surface) may be evaluated prior to beginning the CT simulation procedure in order to gauge dose to the simulation therapists. A departmental policy should be developed on the radiation exposure limit above which certain sensitive workers (e.g., women of child bearing age) may not be allowed to work with the patient. For pediatric patients, radiopharmaceutical dose levels should be carefully considered from the point of view of minimizing the potential risk of secondary cancers.[158] There are numerous factors that directly and indirectly affect patient/staff radiation dose. For a comprehensive treatment of these factors and guidelines for dose management and optimization, the reader is referred to Report No. 58 from the International Atomic Energy Agency.[159] We also note the AAPM Position Statement on Radiation Risks from Medical Imaging Procedures (PP 25-A, 2013, http://www.aapm.org/org/policies/details.asp?xml:id=318&type=PP), which holds that the benefits of imaging should be acknowledged while bearing in mind that the risks are potentially low.

5. SUMMARY OF RECOMMENDATIONS

1. Acceptance testing for PET portion of PET/CT should at least: (a) include NEMA NU 2-2012 performance measures; (b) pass tests on ACR flangeless PET phantom SUV parameters and resolution and/or pass European standards, such as provided by EARL; (c) have acceptable alignment (no offsets or skews) between the PET and CT image sets of the ACR flangeless phantom. Where appropriate, tests from TG-126 (PET/CT Acceptance Testing and Quality Assurance) should be incorporated that either have more stringent criteria than those specified in this report, or do not exist in this report.
2. Compliance with the test specifications used for ACR accreditation or EARL accreditation (EU) is recommended (for acceptance and for subsequent annual QA).
3. Annual QA tests should be performed on the ACR flangeless phantom corresponding to SUV parameters and resolutions (as in ACR accreditation or as in EARL accreditation), and PET/CT alignment.
4. Monthly QA tests should be performed for uniformity, quantification, scatter correction and randoms rejection, resolution, and PET/CT alignment.
5. All tests in 1–4, above, should be performed by a Qualified Medical Physicist (QMP) (refer to American Association of Physicists in Medicine (AAPM) "Definition of a Qualified Medical Physicist"[31]), as appropriate, or individuals working under the general supervision of a QMP ("general supervision" as defined in the AAPM Medical Physics Practice Guideline[32]). The Qualified Medical Physicist should review and approve via countersignature all tests performed by the individual under their supervision.
6. Patient scanning protocol should ensure consistency of patient parameters, radiopharmaceutical activity and administration, immobilization and imaging parameters, as in Table II.
7. Reporting in literature should include key patient and scanning parameters, as in Table III.

8. Treatment planning systems should include: (a) conversion of PET image to SUV and testing of accuracy of SUV calculation; (b) delineation of tumor using SUV cutoff/relative (%) thresholding for target definition/ other sophisticated PET segmentation algorithms, as well as mapping of SUV distribution to radiotherapy inverse planning objectives for dose painting; and (c) support for fusing of multiple FDG-PET datasets (pre, during, posttreatment) and analysis of changes.
9. Rigid registration is recommended when translating information from PET images to CT images used for planning purposes.

The recommendations provided here are minimal requirements and are not meant to cover all aspects of the use of [^{18}F]FDG-PET for RT. The publicly available IAEA staffing needs report for Diagnostic Imaging and Radionuclide Therapy[160] estimates that annual QA and routine quality controls on a PET/CT system require approximately 0.1 of a full time equivalent (FTE) clinically qualified medical physicist. We estimate that the addition of monthly QA will increase the required effort by approximately 12–15 h per year.

CONFLICT OF INTEREST

The authors have no conflicts to disclose.

[a)]Author to whom correspondence should be addressed. Electronic mail: shiva_das@med.unc.edu

REFERENCES

1. Sargos P, Charleux T, Haas RL, et al. Pre- and postoperative radiotherapy for extremity soft tissue sarcoma: Evaluation of inter-observer target volume contouring variability among French sarcoma group radiation oncologists. *Cancer Radiotherapie*. 2018;22:131–139.
2. Onal C, Cengiz M, Guler OC, Dolek Y, Ozkok S. The role of delineation education programs for improving interobserver variability in target volume delineation in gastric cancer. *Br J Radiol*. 2017;90:20160826.
3. Ciardo D, Argenone A, Boboc GI, et al. Variability in axillary lymph node delineation for breast cancer radiotherapy in presence of guidelines on a multi-institutional platform. *Acta Oncol*. 2017;56:1081–1088.
4. Chang ATY, Tan LT, Duke S, Ng WT. Challenges for quality assurance of target volume delineation in clinical trials. *Front Oncol*. 2017;7:221..
5. De Bari B, Dahele M, Palmu M, et al. Short interactive workshops reduce variability in contouring treatment volumes for spine stereotactic body radiation therapy: Experience with the ESTRO FALCON programme and EduCase (TM) training tool. *Radiother Oncol*. 2018;127:150–153.
6. Vinod SK, Jameson MG, Min M, Holloway LC. Uncertainties in volume delineation in radiation oncology: A systematic review and recommendations for future studies. *Radiother Oncol*. 2016;121:169–179.
7. Spoelstra FOB, Senan S, Le Pechoux C, et al. Variations in target volume definition for postoperative radiotherapy in stage III non–small-cell lung cancer: Analysis of an international contouring study. *Int J Radiat Oncol Biol Phys*. 2010;76:1106–1113.
8. Weiss E, Hess CF. The impact of gross tumor volume (GTV) and clinical target volume (CTV) definition on the total accuracy in radiotherapy - Theoretical aspects and practical experiences. *Strahlenther Onkol*. 2003;179:21–30.
9. Li XA, Tai A, Arthur DW, et al. Variability of target and normal structure delineation for breast cancer radiotherapy: an RTOG Multi-institutional and Multiobserver study. *Int J Radiat Oncol Biol Phys*. 2009;73:944–951.
10. Silvestri GA, Gonzalez AV, Jantz MA, et al. Methods for staging non-small cell lung cancer diagnosis and management of lung cancer, 3rd ed: American college of chest Physicians evidence-based clinical practice guidelines. *Chest*. 2013;143:E211–E250.
11. Kinahan PE, Hasegawa BH, Beyer T. X-ray-based attenuation correction for positron emission tomography/computed tomography scanners. *Semin Nucl Med*. 2003;33:166–179.
12. Pohar S, Brown R, Newman N, Koniarczyklow M, Hsu J, Feiglin D. What does pet imaging add to conventional staging of head and neck cancer patients? *Int J Radiat OncolBiolPhys*. 2007;68:383–387.
13. Farina E, Ferioli M, Castellucci P, et al. 18F-Fdg-PET-guided planning and re-planning (Adaptive) radiotherapy in head and neck cancer: current state of art. *Anticancer Res*. 2017;37:6523–6532.
14. Møller DS, Nielsen TB, Brink C, et al. Heterogeneous FDG-guided dose-escalation for locally advanced NSCLC (the NARLAL2 trial): design and early dosimetric results of a randomized, multi-centre phase-III study. *Radiother Oncol*. 2017;124:311–317.
15. Lee E, Zeng J, Miyaoka RS, et al. Functional lung avoidance and response-adaptive escalation (FLARE) RT: Multimodality plan dosimetry of a precision radiation oncology strategy: Multimodality. *Med Phys*. 2017;44:3418–3429.
16. De Ruysscher D, Faivre-Finn C, Moeller D, et al. European Organization for Research and Treatment of Cancer (EORTC) recommendations for planning and delivery of high-dose, high precision radiotherapy for lung cancer. *Radiother Oncol*. 2017;124:1–10.
17. Ford EC, Lavely WC, Frassica DA, et al. Comparison of FDG-PET/CT and CT for delineation of lumpectomy cavity for partial breast irradiation. *Int J Radiat Oncol Biol Phys*. 2008;71:595–602.
18. Davidson T, Ben-David M, Galper S, et al. Use of18F-FDG PET-CT imaging to determine internal mammary lymph node location for radiation therapy treatment planning in breast cancer patients. *Pract Radiat Oncol*. 2017;7:373–381.
19. Beukinga RJ, Hulshoff JB, Mul VEM, et al. Prediction of response to neoadjuvant chemotherapy and radiation therapy with baseline and restaging 18F-FDG PET imaging biomarkers in patients with esophageal cancer. *Radiology*. 2018;287:983–992.
20. Brianzoni E, Rossi G, Ancidei S, et al. Radiotherapy planning: PET/CT scanner performances in the definition of gross tumour volume and clinical target volume. *Eur J Nucl Med Mol Imaging*. 2005;32:1392–1399.
21. Esthappan J, Chaudhari S, Santanam L, et al. Prospective clinical trial of positron emission tomography/computed tomography image-guided intensity-modulated radiation therapy for cervical carcinoma with positive para-aortic lymph nodes. *Int J Radiat Oncol Biol Phys*. 2008;72:1134–1139.
22. Patel DA, Chang ST, Goodman KA, et al. Impact of integrated PET/CT on variability of target volume delineation in rectal cancer. *Technol Cancer Res Treat*. 2007;6:31–36.
23. Ciernik IF, Dizendorf E, Baumert BG, et al. Radiation treatment planning with an integrated positron emission and computer tomography PET/CT: A feasibility study. *Int J Radiat Oncol Biol Phys*. 2003;57:853–863.
24. Li J, Xiao Y. Application of FDG-PET/CT in radiation oncology. *Front Oncol*. 2013;3:80.
25. Niederkohr RD, Greenspan BS, Prior JO, et al. Reporting guidance for oncologic F-18-FDG PET/CT imaging. *J Nucl Med*. 2013;54:756–761.
26. Czernin J, Allen-Auerbach M, Nathanson D, Herrmann K. PET/CT in oncology: current status and perspectives. *Curr Radiol Rep*. 2013;1:177–190.
27. Beyer T, Czernin J, Freudenberg LS. Variations in clinical PET/CT operations: results of an international survey of active PET/CT users. *J Nucl Med*. 2011;52:303–310.
28. Thorwarth D, Beyer T, Boellaard R, et al. Integration of FDG-PET/CT into external beam radiation therapy planning: Technical aspects and recommendations on methodological approaches. *Nuklearmedizin*. 2012;51:140–153.
29. Sattler B, Lee JA, Lonsdale M, Coche E. PET/CT (and CT) instrumentation, image reconstruction and data transfer for radiotherapy planning. *Radiother Oncol*. 2010;96:288–297.

30. Boellaard R, O'Doherty MJ, Weber WA, et al. FDG PET and PET/CT: EANM procedure guidelines for tumour PET imaging: version 1.0. *Eur J Nucl Med Mol Imaging*. 2010;37:181–200.
31. AAPM. Definition of a Qualified Medical Physicist. https://www.aapm.org/org/policies/details.asp?xml:id=449 (accessed date 22 July, 2019).
32. Clements JB, Baird CT, de Boer SF, et al. AAPM medical physics practice guideline 10.a.: scope of practice for clinical medical physics. *J Appl Clin Med Phys*. 2018;19:11–25.
33. Cherry SR, Phelps ME, Sorenson JA. *Physics in Nuclear Medicine*. Philadelphia: Elsevier/Saunders; 2012.
34. Tong S, Alessio AM, Kinahan PE. Noise and signal properties in PSF-based fully 3D PET image reconstruction: an experimental evaluation. *Phys Med Biol*. 2010;55:1453–1473.
35. Matheoud R, Ferrando O, Valzano S, et al. Performance comparison of two resolution modeling PET reconstruction algorithms in terms of physical figures of merit used in quantitative imaging. *Phys. Medica*. 2015;31:468–475.
36. van der Vos CS, Koopman D, Rijnsdorp S, et al. Quantification, improvement, and harmonization of small lesion detection with state-of-the-art PET. *Eur J Nucl Med Mol Imaging*. 2017;44:S4–S16.
37. Tong S, Alessio AM, Thielemans K, Stearns C, Ross S, Kinahan PE. Properties and mitigation of edge artifacts in PSF-based PET reconstruction. *IEEE Trans Nucl Sci*. 2011;58:2264–2275.
38. Lasnon C, Desmonts C, Quak E, et al. Harmonizing SUVs in multicentre trials when using different generation PET systems: prospective validation in non-small cell lung cancer patients. *Eur J Nucl Med Mol Imaging*. 2013;40:985–996.
39. Czernin J, Schelbert H. PET/CT imaging: facts, opinions, hopes, and questions. *J Nucl Med*. 2004; 45:1S–3.
40. Drzezga A, Souvatzoglou M, Eiber M, et al. First clinical experience with integrated whole-body PET/MR: comparison to PET/CT in patients with oncologic diagnoses. *J Nucl Med*. 2012;53:845–855.
41. Leibfarth S, Eckert F, Welz S, et al. Automatic delineation of tumor volumes by co-segmentation of combined PET/MR data. *Phys Med Biol*. 2015;60:5399–5412.
42. Spick C, Herrmann K, Czernin J. F-18-FDG PET/CT and PET/MRI perform equally well in cancer: evidence from studies on more than 2,300 patients. *J Nucl Med*. 2016;57:420–430.
43. Osborne DR, Acuff S, Cruise S, et al. Quantitative and qualitative comparison of continuous bed motion and traditional step and shoot PET/CT. *Am J Nucl Med Mol Imaging*. 2015;5:56–64.
44. Schatka I, Weiberg D, Reichelt S, et al. A randomized, double-blind, crossover comparison of novel continuous bed motion versus traditional bed position whole-body PET/CT imaging. *Eur J Nucl Med Mol Imaging*. 2016;43:711–717.
45. Cherry SR, Jones T, Karp JS, Qi JY, Moses WW, Badawi RD. Total-Body PET: maximizing sensitivity to create new opportunities for clinical research and patient care. *J Nucl Med*. 2018;59:3–12.
46. Hany TF, Steinert HC, Goerres GW, Buck A, von Schulthess GK. PET diagnostic accuracy: improvement with in-line PET-CT system: initial results. *Radiology*. 2002;225:575–581.
47. Cherry SR, Sorenson JA, Phelps ME. *Physics in Nuclear Medicine (Third Edition)*. Philadelphia, PA: Saunders; 2003:377–403.
48. Kim CK, Gupta NC, Chandramouli B, Alavi A. Standardized uptake values of FDG: body surface area correction is preferable to body weight correction. *J Nucl Med*. 1994;35:164–167.
49. Tahari AK, Chien D, Azadi JR, Wahl RL. Optimum lean body formulation for correction of standardized uptake value in PET imaging. *J Nucl Med : official publication, Society of Nuclear Medicine*. 2014;55:1481–1484.
50. Beaulieu S, Kinahan P, Tseng J, et al. SUV varies with time after injection in F-18-FDG PET of breast cancer: Characterization and method to adjust for time differences. *J Nucl Med*. 2003;44:1044–1050.
51. Hamberg LM, Hunter GJ, Alpert NM, Choi NC, Babich JW, Fischman AJ. The dose uptake ratio as an index of glucose metabolism: useful parameter or oversimplification? *J Nucl Med*. 1994;35:1308–1312.
52. van den Hoff J, Lougovski A, Schramm G, et al. Correction of scan time dependence of standard uptake values in oncological PET. *Ejnmmi Res*. 2014;4:1–14.
53. Langen KJ, Braun U, Rota Kops E, et al. The influence of plasma glucose levels on fluorine-18-fluorodeoxyglucose uptake in bronchial carcinomas. *J Nucl Med*. 1993;34:355–359.
54. Claeys J, Mertens K, D'Asseler Y, Goethals I. Normoglycemic plasma glucose levels affect F-18 FDG uptake in the brain. *Ann Nucl Med*. 2010;24:501–505.
55. Keyes JW Jr. SUV: standard uptake or silly useless value? *J Nucl Med*. 1995;36(10):1836–1839.
56. Kinahan PE, Fletcher JW. Positron emission tomography-computed tomography standardized uptake values in clinical practice and assessing response to therapy. *Seminars in Ultrasound Ct and Mri*. 2010;31:496–505.
57. Adams MC, Turkington TG, Wilson JM, Wong TZ. A Systematic review of the factors affecting accuracy of SUV measurements. *Am J Roentgenol*. 2010;195:310–320.
58. Galavis PE, Hollensen C, Jallow N, Paliwal B, Jeraj R. Variability of textural features in FDG PET images due to different acquisition modes and reconstruction parameters. *Acta oncologica (Stockholm, Sweden)*. 2010;49:1012–1016.
59. Nehmeh SA, Erdi YE, Ling CC, et al. Effect of respiratory gating on reducing lung motion artifacts in PET imaging of lung cancer. *Med Phys*. 2002;29:366–371.
60. Boellaard R, Krak NC, Hoekstra OS, Lammertsma AA. Effects of noise, image resolution, and ROI definition on the accuracy of standard uptake values: a simulation study. *J Nucl Med*. 2004;45:1519–1527.
61. FDG-PET/CT Technical Committee. FDG-PET/CT as an imaging biomarker measuring response to cancer therapy, Quantitative Imaging Biomarkers Alliance, Version 1.05, Publicly Reviewed Version. QIBA, December 11, 2013. Available from RSNA.ORG/QIBA.
62. Hellwig D, Graeter TP, Ukena D, et al. 18F-FDG PET for mediastinal staging of lung cancer: which SUV threshold makes sense? *J Nucl Med*. 2007;48:1761–1766.
63. Al-Sarraf N, Gately K, Lucey J, et al. Clinical implication and prognostic significance of standardised uptake value of primary non-small cell lung cancer on positron emission tomography: analysis of 176 cases. *Eur J Cardiothorac Surg*. 2008;34:892–897.
64. Oshida M, Uno K, Suzuki M, et al. Predicting the prognoses of breast carcinoma patients with positron emission tomography using 2-deoxy-2-fluoro[18F]-D-glucose. *Cancer*. 1998;82:2227–2234.
65. Meirelles GS, Schoder H, Ravizzini GC, et al. Prognostic value of baseline [18F] fluorodeoxyglucose positron emission tomography and 99mTc-MDP bone scan in progressing metastatic prostate cancer. *Clin Cancer Res*. 2010;16:6093–6099.
66. Eary JF, O'Sullivan F, Powitan Y, et al. Sarcoma tumor FDG uptake measured by PET and patient outcome: a retrospective analysis. *Eur J Nucl Med Mol Imaging*. 2002;29:1149–1154.
67. Pryma DA, Schoder H, Gonen M, Robbins RJ, Larson SM, Yeung HW. Diagnostic accuracy and prognostic value of 18F-FDG PET in Hurthle cell thyroid cancer patients. *J Nucl Med*. 2006;47:1260–1266.
68. MacManus M, Nestle U, Rosenzweig KE, et al. Use of PET and PET/CT for radiation therapy planning: IAEA expert report 2006–2007. *Radiother Oncol*. 2009;91:85–94.
69. Cacicedo J, Fernandez I, del Hoyo O, et al. Should PET/CT be implemented in the routine imaging work-up of locally advanced head and neck squamous cell carcinoma? A prospective analysis. *Eur J Nucl Med Mol Imaging*. 2015;42:1378–1389.
70. Bradley J, Thorstad WL, Mutic S, et al. Impact of FDG-PET on radiation therapy volume delineation in non-small-cell lung cancer. *Int J Radiat Oncol Biol Phys*. 2004;59:78–86.
71. Czernin J, Phelps ME. Positron emission tomography scanning: current and future applications. *Annu Rev Med*. 2002;53:89–112.
72. Almuhaideb A, Papathanasiou N, Bomanji J. 18F-FDG PET/CT imaging in oncology. *Ann Saudi Med*. 2011;31:3–13.
73. International Commission on Radiation Units & Measurement. ICRU Report 50—Prescribing, Recording and Reporting Photon Beam Therapy Bethesda, MD: ICRU Publications; 1993
74. Erdi Y, Rosenzweig K, Erdi A. Radiotherapy treatment planning for patients with NSCLC using PET. *Radiother Oncol*. 2002;62:51–60.
75. Koshy M, Paulino AC, Howell R, Schuster D, Halkar R, Davis LW. F-18 FDG PET-CT fusion in radiotherapy treatment planning for head and neck cancer. *Head Neck*. 2005;27:494–502.
76. Boellaard R. Standards for PET image acquisition and quantitative data analysis. *J Nucl Med*. 2009;50:11S–20S.

77. Berthon B, Spezi E, Galavis P, et al. Toward a standard for the evaluation of PET-Auto-Segmentation methods following the recommendations of AAPM task group No. 211: Requirements and implementation. *Med Phys*. 2017;44:4098–4111.
78. Erdi YE, Mawlawi O, Larson SM, et al. Segmentation of lung lesion volume by adaptive positron emission tomography image thresholding. *Cancer*. 1997;80:S2505–S2509.
79. Meignan M, Sasanelli M, Casasnovas RO, et al. Metabolic tumour volumes measured at staging in lymphoma: methodological evaluation on phantom experiments and patients. *Eur J Nucl Med Mol Imaging*. 2014;41:1113–1122.
80. Patz EF, Lowe VJ, Hoffman JM, Paine SS, Harris LK, Goodman PC. Persistent or recurrent bronchogenic-carcinoma - detection with PET and 2- F-18 -2-Deoxy-D-Glucose. *Radiology*. 1994;191:379–382.
81. Cheebsumon P, van Velden FHP, Yaqub M, et al. Effects of image characteristics on performance of tumor delineation methods: a test-retest assessment. *J Nucl Med*. 2011;52:1550–1558.
82. Konert T, Vogel W, MacManus MP, et al. PET/CT imaging for target volume delineation in curative intent radiotherapy of non-small cell lung cancer: IAEA consensus report 2014. *Radiother Oncol*. 2015;116:27–34.
83. Nestle U, Kremp S, Schaefer-Schuler A, e. al. Comparison of different methods for delineation of 18F-FDG PET–positive tissue for target volume definition in radiotherapy of patients with non–small cell lung cancer. *J Nucl Med*. 2005;46:1342–1348.
84. Black QC, Grills IS, Kestin LL, e. al. Defining a radiotherapy target with positron emission tomography. *Int J Radiat Oncol Biol Phys*. 2004;60:1272–1282.
85. Jentzen W, Freudenberg L, Eising EG, Heinze M, Brandau W, Bockisch A. Segmentation of PET volumes by iterative image thresholding. *J Nucl Med*. 2007;48:108–114.
86. Werner-Wasik M, Nelson AD, Choi W, et al. What is the best way to contour lung tumors on PET scans? Multiobserver validation of a gradient-based method using a NSCLC digital PET phantom. *Int J Radiat Oncol Biol Phys*. 2012;82:1164–1171.
87. Geets X, Lee JA, Bol A, Lonneux M, Gregoire V. A gradient-based method for segmenting FDG-PET images: methodology and validation. *Eur J Nucl Med Mol Imaging*. 2007;34:1427–1438.
88. Li H, Thorstad WL, Biehl KJ, et al. A novel PET tumor delineation method based on adaptive region-growing and dual-front active contours. *Med Phys*. 2008;35:3711–3721.
89. McGurk RJ, Bowsher J, Lee JA, Das SK. Combining multiple FDG-PET radiotherapy target segmentation methods to reduce the effect of variable performance of individual segmentation methods. *Med Phys*. 2013;40:042501.
90. Bagci U, Udupa JK, Mendhiratta N, et al. Joint segmentation of anatomical and functional images: applications in quantification of lesions from PET, PET-CT, MRI-PET, and MRI-PET-CT images. *Med Image Anal*. 2013;17:929–945.
91. Song Q, Bai J, Han D, et al. Optimal co-segmentation of tumor in PET-CT images with context information. *IEEE Trans Med Imaging*. 2013;32:1685–1697.
92. Schaefer A, Vermandel M, Baillet C, et al. Impact of consensus contours from multiple PET segmentation methods on the accuracy of functional volume delineation. *Eur J Nucl Med Mol Imaging*. 2016;43:911–924.
93. Lu W, Olivera GH, Chen Q, Chen ML, Ruchala KJ. Automatic re-contouring in 4D radiotherapy. *Phys Med Biol*. 2006;51:1077–1099.
94. Differding S, Sterpin E, Janssens G, Hanin FX, Lee JA, Grégoire V. Methodology for adaptive and robust FDG-PET escalated dose painting by numbers in head and neck tumors. *Acta Oncol*. 2016;55:217–225.
95. Raman S, Bissonnette JP, Warner A, et al. Rationale and Protocol for a Canadian Multicenter Phase II Randomized Trial Assessing Selective Metabolically Adaptive Radiation Dose Escalation in Locally Advanced Non–small-cell Lung Cancer (NCT02788461). *Clin Lung Cancer*. 2018;19:e699–e703.
96. Berwouts D, Madani I, Duprez F, et al. Long-term outcome of 18F-fluorodeoxyglucose-positron emission tomography-guided dose painting for head and neck cancer: matched case-control study. *Head Neck*. 2017;39:2264–2275.
97. Frood R, Prestwich R, Tsoumpas C, Murray P, Franks K, Scarsbrook A. Effectiveness of respiratory-gated positron emission tomography/computed tomography for radiotherapy planning in patients with lung carcinoma – A systematic review. *Clin Oncol (R Coll Radiol)*. 2018;30:225–232.
98. Kishi T, Matsuo Y, Nakamura A, et al. Comparative evaluation of respiratory-gated and ungated FDG-PET for target volume definition in radiotherapy treatment planning for pancreatic cancer. *Radiother Oncol*. 2016;120:217–221.
99. Sindoni A, Minutoli F, Pontoriero A, Iatì G, Baldari S, Pergolizzi S. Usefulness of four dimensional (4D) PET/CT imaging in the evaluation of thoracic lesions and in radiotherapy planning: review of the literature. *Lung Cancer*. 2016;96:78–86.
100. Brock KK, Mutic S, McNutt TR, Li H, Kessler ML. Use of image registration and fusion algorithms and techniques in radiotherapy: report of the AAPM radiation therapy committee task. *Med Phys*. 2017;44:E43–E76.
101. Bajcsy R, Kovacic S. Multiresolution elastic matching. *Comput Vis, Graph Image Process*. 1989;46:1–21.
102. Gee JC, Haynor DR, Reivich M, Bajcsy R. Finite element approach to warping of brain images. *Proc, SPIE Medical Imaging*. 1994;2167:18–27.
103. Gee JC, Reivich M, Bajcsy R. Elastically deforming 3D atlas to match anatomical brain images. *J Comput Assist Tomogr*. 1993;17:225–236.
104. Christensen GE, Rabitt RD, Miller MI. Deformable templates using large deformable kinematics. *IEEE Trans Med Imaging*. 1996;5:1435–1447.
105. Thirion J-P. Image matching as a diffusion process: an analogy with Maxwell's demons. *Med Image Anal*. 1998;2:18.
106. Thirion JP. Image matching as the diffusion process: an analogy wth Maxwell's demons. *Med Image Anal*. 1998;2:243–260.
107. Huang TC, Zhang G, Guerrero T, Starkschall G, Lin KP, Forster K. Semi-automated CT segmentation using optic flow and Fourier interpolation techniques. *Comput Meth Prog Bio*. 2006;84:124–134.
108. Wang H, Dong L, Lii MF, et al. Implementation and validation of a three-dimensional deformable registration algorithm for targeted prostate cancer radiotherapy. *Int J Radiat Oncol Biol Phys*. 2005;61:725–735.
109. Brock KM, Balter JM, Dawson LA, Kessler ML, Meyer CR. Automated generation of a four-dimensional model of the liver using warping and mutual information. *Med Phys*. 2003;30:1128–1133.
110. Schreibmann E, Xing L. Image registration with auto-mapped control volumes. *Med Phys*. 2006;33:1165–1179.
111. Schreibmann E, Yang Y, Boyer A, Li T, Xing L. Image interpolation in 4D CT using a BSpline deformable registration model. *Med Phys*. 2005;32:1924.
112. Coselmon MM, Balter JM, McShan DL, Kessler ML. Mutual information based CT registration of the lung at exhale and inhale breathing states using thin-plate splines. *Med Phys*. 2004;31:2942.
113. Bookstein FL. Principal warps - thin-plate splines and the decomposition of deformations. *IEEE Trans Pattern Anal Mach Intell*. 1989;11:567–585.
114. Lian J, Xing L, Hunjan S, et al. Mapping of the prostate in endorectal coil-based MRI/MRSI and CT: a deformable registration and validation study. *Med Phys*. 2004;31:3087–3094.
115. Brock KK, Hollister SJ, Dawson LA, Balter JM. Technical note: creating a four-dimensional model of the liver using finite element analysis. *Med Phys*. 2002;29:1403–1405.
116. Fei B, Kemper C, Wilson DL. A comparative study of warping and rigid body registration for the prostate and pelvic MR volumes. *Comp Med Imag Graph*. 2003;4:267–281.
117. Jani SS, Robinson CG, Dahlbom M, et al. A Comparison of amplitude-based and phase-based positron emission tomography gating algorithms for segmentation of internal target volumes of tumors subject to respiratory motion. *Int J Radiat Oncol Biol Phys*. 2013;87:562–569.
118. Pepin A, Daouk J, Bailly P, Hapdey S, Meyer ME. Management of respiratory motion in PET/computed tomography: the state of the art. *Nucl Med Commun*. 2014;35:113–122.
119. Buther F, Vehren T, Schafers KP, Schafers M. Impact of data-driven respiratory gating in clinical PET. *Radiology*. 2016;281:229–238.

120. Schleyer PJ, O'Doherty MJ, Barrington SF, Marsden PK. Retrospective data-driven respiratory gating for PET/CT. *Phys Med Biol*. 2009;54:1935–1950.
121. Bentzen SM, Gregoire V. Molecular imaging-based dose painting: a novel paradigm for radiation therapy prescription. *Semin Radiat Oncol*. 2011;21:101–110.
122. Aerts H, Lambin P, De Ruysscher D. FDG for dose painting: a rational choice. *Radiother Oncol*. 2010;97:163–164.
123. Meijer G, Steenhuijsen J, Bal M, De Jaeger K, Schuring D, Theuws J. Dose painting by contours versus dose painting by numbers for stage II/III lung cancer: practical implications of using a broad or sharp brush. *Radiother Oncol*. 2011;100:396–401.
124. Vanderstraeten B, Duthoy W, De Gersem W, De Neve W, Thierens H. F-18 fluoro-deoxy-glucose positron emission tomography (F-18 FDG-PET) voxel intensity-based intensity-modulated radiation therapy (IMRT) for head and neck cancer. *Radiother Oncol*. 2006;79:249–258.
125. Das SK, Miften MM, Zhou S, et al. Feasibility of optimizing the dose distribution in lung tumors using fluorine-18-fluorodeoxyglucose positron emission tomography and single photon emission computed tomography guided dose prescriptions. *Med Phys*. 2004;31:1452–1461.
126. Alber M, Paulsen F, Eschmann SM, Machulla HJ. On biologically conformal boost dose optimization. *Phys Med Biol*. 2003;48:N31–35.
127. Geets X, Tomsej M, Lee JA, et al. Adaptive biological image-guided IMRT with anatomic and functional imaging in pharyngo-laryngeal tumors: impact on target volume delineation and dose distribution using helical tomotherapy. *Radiother Oncol*. 2007;85:105–115.
128. Aerts H, Bosmans G, van Baardwijk AAW, et al. Stability of F-18-deoxyglucose uptake locations within tumor during radiotherapy for NSCLC: a prospective study. *Int J Radiat Oncol Biol Phys*. 2008;71:1402–1407.
129. La Fontaine M, Vogel W, van Diessen J, et al. A secondary analysis of FDG spatio-temporal consistency in the randomized phase II PET-boost trial in stage II-III NSCLC. *Radiother Oncol*. 2018;127:259–266.
130. van Elmpt W, De Ruysscher D, van der Salm A, et al. The PET-boost randomised phase II dose-escalation trial in non-small cell lung cancer. *Radiother Oncol*. 2012;104:67–71.
131. Garibaldi C, Ronchi S, Cremonesi M, et al. Interim F-18-FDG PET/CT during chemoradiation therapy in the management of head and neck cancer patients: a systematic review. *Int J Radiat Oncol Biol Phys*. 2017;98:555–573.
132. Min M, Lin P, Liney G, et al. A review of the predictive role of functional imaging in patients with mucosal primary head and neck cancer treated with radiation therapy. *J Med Imaging Radiat Oncol*. 2017;61:99–123.
133. Castelli J, De Bari B, Depeursinge A, et al. Overview of the predictive value of quantitative 18 FDG PET in head and neck cancer treated with chemoradiotherapy. *Crit Rev Oncol Hematol*. 2016;108:40–51.
134. Scalco E, Rizzo G. Texture analysis of medical images for radiotherapy applications. *Br J Radiol*. 2017;90:20160642.
135. Cremonesi M, Garibaldi C, Timmerman R, et al. Interim F-18-FDG-PET/CT during chemo-radiotherapy in the management of oesophageal cancer patients. A systematic review. *Radiother Oncol*. 2017;125:200–212.
136. Lu J, Sun XD, Yang X, et al. Impact of PET/CT on radiation treatment in patients with esophageal cancer: a systematic review. *Crit Rev Oncol Hematol*. 2016;107:128–137.
137. Konert T, van de Kamer JB, Sonke JJ, Vogel WV. The developing role of FDG PET imaging for prognostication and radiotherapy target volume delineation in non-small cell lung cancer. *J Thorac Dis*. 2018;10: S2508–S2521.
138. Phillips I, Ajaz M, Ezhil V, et al. Clinical applications of textural analysis in non-small cell lung cancer. *Br J Radiol*. 2018;91:20170267.
139. Amit A, Person O, Keidar Z. FDG PET/CT in monitoring response to treatment in gynecological malignancies. *Curr Opin Obstet Gynecol*. 2013;25:17–22.
140. Association National Electrical Manufacturers. 2018, Vol. NEMA NU 2-2018 (Document ID: 100112).
141. National Electrical Manufacturers Association. Arlington: National Electrical Manufacturers Association. https://www.nema.org/Standards/Pages/Performance-Measurements-of-Positron-Emission-Tomographs.aspx (accessed date 26 July, 2019)
142. Society of Nuclear Medicine and Molecular Imaging. 2017. http://snmmi.files.cms-plus.com/docs/CTN/CTN%20Scanner%20Validation%20Flyer_DoubleSide_FINAL.pdf (accessed date 26 July, 2019)
143. ACR-AAPM. *Technical standard for medical physics performance monitoring of pet/ct imaging equipment*.2018. https://www.acr.org/-/media/ACR/Files/Practice-Parameters/PET-CT-Equip.pdf (accessed date 26 July, 2019)
144. I. A. E. Agency. *Quality Assurance for PET and PET/CT Systems*. Vienna: International Atomic Energy Agency; 2009.
145. Bergmann H, Dobrozemsky G, Minear G, Nicoletti R, Samal M. An inter-laboratory comparison study of image quality of PET scanners using the NEMA NU 2–2001 procedure for assessment of image quality. *Phys Med Biol*. 2005;50:2193–2207.
146. Xing L. Quality assurance of positron emission tomography/computed tomography for radiation therapy. *Int J Radiat Oncol Biol Phys*. 2008;71:S38–S42.
147. Schultheiss TE, Boyer AL, Horton JL, Gastorf RJ. Calibration frequency as determined by analysis of machine stability. *Med Phys*. 1989;16:84–87.
148. Rozenfeld M, Jette D. Quality assurance of radiation dosage: usefulness of redundancy. *Radiology.* 1984;150:241–244.
149. Pawlicki T, Whitaker M, Boyer AL. Statistical process control for radiotherapy quality assurance. *Med Phys*. 2005;32:2777–2786.
150. Huq MS, Fraass BA, Dunscombe PB, et al. The report of Task Group 100 of the AAPM: application of risk analysis methods to radiation therapy quality management. *Med Phys*. 2016;43:4209–4262.
151. Mutic S, Palta JR, Butker EK, et al. Quality assurance for computed-tomography simulators and the computedtomography-simulation process: report of the AAPM radiation therapy committee task group no. 66. *Med Phys*. 2003;30:2762–2792.
152. Delbeke D, Coleman RE, Guiberteau MJ, et al. Procedure guideline for tumor imaging with 18F-FDG PET/CT 1.0. *J Nucl Med*. 2006;47:885–895.
153. Shankar LK, Hoffman JM, Bacharach S, et al. Consensus recommendations for the use of F-18-FDG PET as an indicator of therapeutic response in patients in national cancer institute trials. *J Nucl Med*. 2006;47:1059–1066.
154. Kinahan P, Pierce L, Elston B, Clunie D, Nelson D. An FDG-PET/CT digital reference object for testing ROI and SUV calculations. *J Nucl Med*. 2012;53:607–607.
155. Hatt M, Laurent B, Ouahabi A, et al. The first MICCAI challenge on PET tumor segmentation. *Med Image Anal*. 2018;44:177–195.
156. Madsen MT, Anderson JA, Halama JR, et al. AAPM task group 108: PET and PET/CT shielding requirements. *Med Phys*. 2006;33:4–15.
157. Xia T, Alessio AM, De Man B, Manjeshwar R, Asma E, Kinahan PE. Ultra-low dose CT attenuation correction for PET/CT. *Phys Med Biol*. 2012;57:309–328.
158. Kaste SC. PET-CT in children: where is it appropriate? *Pediatr Radiol*. 2011;41:509–513.
159. IAEA. Radiation Protection in Newer Medical Imaging Techniques: PET/CT (Safety Reports Series No. 58). 2008.
160. International Atomic Energy Agency. Medical physics staffing needs in diagnostic imaging and radionuclide therapy: An Activity based approach, Iaea human health reports no. 15. Vienna: International Atomic Energy Agency; 2018.

SUPPORTING INFORMATION

Additional supporting information may be found online in the Supporting Information section at the end of the article.

Appendix. S1: Monthly Quality Assurance of PET/CT.
Appendix. S2: Example PET/CT simulation protocol for RT planning.

BEAMSCAN® MR

STARCHECK*maxi*® MR

PRECISION MR-LINAC QA

New PTW technology delivers improved treatment success and patient safety in MR-guided radiotherapy. The **BEAMSCAN® MR*** motorized 3D water phantom – available in two models for Elekta Unity and ViewRay® MRIdian® – provides a dedicated, fully equipped solution for beam data commissioning and QA of MR-LINACs. The **STARCHECK*maxi*® MR** ionization chamber array provides comprehensive MR-LINAC QA with one single device and outstanding accuracy. One shot delivers all relevant beam data at 3 mm spatial resolution for radiation fields up to 40 x 40 cm^2.

Contact PTW today, and take a closer look at all the ways we can support your dosimetry needs for MR-guided radiotherapy.

(516) 827-3181 • www.MRdosimetry.com

PTW THE DOSIMETRY COMPANY

*Pending 510(k), not available for sale within the United States.